ADDIS ABABA UNIVERSITY

ADDIS ABABA INSTITUTE OF TECHNOLOGY

SCHOOL OF MULTIDISCIPLINARY ENGINEERING

CENTER FOR MATERIALS ENGINEERING

Synthesis and Characterization of Titanium Dioxide Immobilized Water Hyacinth based Activated Carbon Catalyst for Methylene Blue Removal

ABEBAYEHU KEFYALEW

A Thesis Submitted to the Center for Materials Engineering, School of Multidisciplinary Engineering, Addis Ababa Institute of Technology, Addis Ababa University in Partial Fulfillment of the Requirements for the Degree of Master of Science in Materials Engineering

ADDIS ABABA UNIVERSITY

ADDIS ABABA, ETHIOPIA

August 2021

ADDIS ABABA UNIVERSITY

ADDIS ABABA INSTITUTE OF TECHNOLOGY

SCHOOL OF MULTIDISCIPLINARY ENGINEERING

CENTER FOR MATERIALS ENGINEERING

Synthesis and Characterization of Titanium Dioxide Immobilized Water Hyacinth based Activated Carbon Catalyst for Methylene Blue Removal

ABEBAYEHU KEFYALEW AKLOG

A Thesis Submitted to the Center for Materials Engineering, School of Multidisciplinary Engineering, Addis Ababa Institute of Technology, Addis Ababa University in Partial Fulfillment of the Requirements for the Degree of Master of Science in Materials Engineering

August 2021

ADDIS ABABA UNIVERSITY

ADDIS ABABA INSTITUTE OF TECHNOLOGY

SCHOOL OF MULTIDISCIPLINARY ENGINEERING

CENTER FOR MATERIALS ENGINEERING

This is to certify that the thesis prepared by **Abebayehu Kefyalew** entitled **"Synthesis and Characterization of Titanium Dioxide Immobilized on Water Hyacinth based Activated Carbon Catalyst for Methyleneblue Removal"** submitted in partial fulfillment of the requirements for the Degree of Master of Science in Materials Engineering complies with the regulations of the university and meets the accepted standards concerning originality and quality.

Approved by Board of Examiners

Internal Examiner	**Signature**	**Date**
External Examiner	**Signature**	**Date**
Advisor	**Signature**	**Date**
Co-advisor	**Signature**	**Date**
Centre Head	**Signature**	**Date**

DECLARATION

I hereby declare that this M.Sc. thesis is my original work and has not been previously submitted partially or in full for an award of a degree in any other university/institution, and all sources of material used in this thesis have been duly acknowledged.

Name **Abebayehu Kefyalew**

Signature _____

Date _____

ABSTRACT

Several treatment methods are available to remove pollutant dyes from textile wastewater streams. Adsorption of pollutant dyes by activated carbon (AC) is one of the technically feasible and cost-effective methods. Incorporating photocatalytic materials such as TiO_2 in AC can improve removal efficiency by imparting photodegradation besides adsorption. In this study, titanium dioxide-immobilized water hyacinth-based activated carbon catalyst (TiO_2/WHAcc) was used to remove Methylene blue (MB) from artificially constituted wastewater. The AC extracted from lignocellulosic biomass was utilized to adsorb MB and further impregnation of AC with TiO_2 enhanced the MB removal efficiency. The source of lignocellulosic biomass in this work was water hyacinth biomass (WHB). Sol-gel method was employed to synthesize TiO_2/WHAcc. The WHAC and TiO_2/WHAcc were characterized using X-ray diffraction (XRD), Fourier transform infrared spectroscopy (FT-IR), Brunauer-Emmett-Teller (BET) surface area analysis, and Barrett-Joyner-Halenda (BJH) pore size and volume analysis, field emission scanning electron microscopy equipped with Energy Dispersive x-ray spectroscopy (FE-SEM with EDX), and proximate analyses. In addition, the effect of photocatalytic parameters was investigated using Box-Behnken Design (BBD) response surface methodology. Effects of initial MB dye concentration, catalyst dose, and contact time on percentage removal of MB were studied. The maximum MB removal efficiency of 91.05 % was recorded at 0.092 g adsorbent dosage in 100 ml MB dye solution, 24.58 min contact time, and a MB dye concentration of 20.00 mg L^{-1}. The comparison of TiO_2/WHAcc and WHAC on the removal of MB revealed that the incorporation of TiO_2 in the WHAC enhances the MB removal efficiency and can be a good adsorbent for the removal of MB from wastewater streams.

Keywords: Activated carbon, Methylene blue, Photocatalytic degradation, Titanium dioxide, Water hyacinth

ACKNOWLEDGEMENT

First, I would like to thank the Almighty God, for his invisible hands supporting me throughout the research works and studies.

I would like to express my deepest gratitude to my supervisors Dr. Anteneh Marelign and Dr. Shimeles Kebede for their support, guidance, encouragement, and patience during the hard times in the research work, and also for the theoretical and practical knowledge, they gave me during the entire M.Sc. classes, and especially for their very strong strive of teaching and guiding me and became competent in my profession.

Next, I would like to forward my gratitude to the Head of Center for Materials Engineering, Dr. Sintayehu Nibret, for his encouragement, guidance, supports, facilitating everything without limitation in the Center. I would also like to thank Dr. Dawit Ayana for his encouragement, guidance, and support. I would also like to thank Addis Ababa University for giving me a female scholarship opportunity. I would also like to forward this gratitude to Mr. Zinabu Tasew, academic staff at the School of Chemical and Bio-Engineering, for his support in the compilation of this document.

I would like to forward this gratitude to Mr. Hintsa Selassie Seifu, Mr. Alene, and Engineer Esknder Maseresha, for their strong commitments in assisting me during the experimental work of the research. I would also like to forward my special gratitude to my family, especially to my father Kefyalew Aklog, my mother Azebeb Belay, my sister Betelhem Kefyalew, and my cousin Aderaw Ayalew, and my aunt Tiruy Aklog for their invaluable and continuous supports and encouragements during the whole research work. I would also like to give my gratitude to all my friends, Mariamsina Kasahun, Tariku Tenaye, Demeke, and Addis Tsige, for helping me during the hard times and for encouragement. Above all, I would like to highly acknowledge the School of Chemical and Bio-Engineering of Addis Ababa University and Addis Ababa Science and Technology University for allowing me to use their laboratory facilities.

LIST OF ABBREVIATIONS

AC	Activated Carbon
ASTM	American Society for Testing and Materials
ANOVA	Analysis of Variance
BBD	Box- Behnken-Design
BET	Brunauer-Emmett-Teller
BJH	Barrett-Joyner-Halenda
EDX	Energy Dispersive X-ray Spectroscopy
FE-SEM	Field Emission Scanning Electron Microscope
FTIR	Fourier Transform Infrared Spectroscopy
ICDD	International Center for Diffraction Data
JCPDS	Joint Committee on Powder Diffraction Standards
TiO_2/WHAcc catalyst	Titanium dioxide-immobilized water hyacinth-based activated carbon
WH	Water Hyacinth
WHB	Water Hyacinth Biomass
WHAC	Water Hyacinth based Activated Carbon
WHAcc	Water Hyacinth based Activad Carbon Catalyst

TABLE OF CONTENTS

LIST OF TABLES

LIST OF FIGURES

CHAPTER ONE

1. INTRODUCTION

1.1 Background of the Study

Water is a basic need for all life forms and the quality of water is the most potent and plays a critical role in the survival of human beings. About 70% of the earth's surface is covered with water [1]. Approximately 4 billion people-one half of the world's population will live under conditions of severe water stress in 2025, with conditions, particularly severe in Africa, the Middle East, and South Asia [2]. The major pollutants of the ecosystems are organic and inorganic pollutants [3].

Dyes are a kind of organic compound with a complex aromatic molecular structure that gave bright and firm color to other substances. They are produced in millions of tones every year. There are more than 100,000 commercially available dyes with over 7×10^5 metric tons of dyestuff are produced annually in the world [4]. Synthetic dyes have many applications in various industries such as in leather, textile, food, paper, plastics, cosmetics, and pharmaceuticals. Among many industries, the textile industries use 10-15% of the dye in the manufacturing of textile products, and released into the environment worldwide annually [5]. However, the complex aromatic molecular structure of dyes makes them more stable, difficult to biodegrade, and highly toxic [6]. The textile dyes, along with a large number of industrial pollutants, are highly toxic and potentially carcinogenic, so that they are related to environmental degradation and various diseases in animals and humans [7]. Ethiopia's long history in textile began in 1939 when the first garment factory was established and, the textile, and apparel industry has grown at an average of 51% in the last few years [8].

Color removal from textile dyeing effluents has been the target of great attention not only because of its toxicity but mainly due to its aesthetic effect. Especially when even just 1.0 mg/L of dye concentration in the water supply, it could be inappropriate for human consumption [9]. WH (Emboch) with the scientific name *Eichhornia Crassipes* is a free-floating perennial herb plant often found in a freshwater ecosystem with lavender flowers, dark, thick leaves that flatten out to make a mat on top of the water [10]. It is estimated that 10 plants can produce a mat of 650,000 in one growing season [11]. The plant emerged from Amazon Basin, South America in 1823s [12]. The weed has been distributed around the world and is categorized as one of the worst aquatic weeds in the world [13]. In Africa, WH was first presented in Egypt in 1880 and, in Ethiopia, WH has been realized as the most damaging weed since 1965 [14]. It is also perceptible

in Koka Lake and Awash River. Lake Tana was invaded in 2011 and WH has brought ecological problems. WH lowers light, oxygen, changes water chemistry, and causes a huge increase in water loss due to evapotranspiration. It causes a serious impact on social and economic aspects; also causes a critical problem in marine transportation, fishing, hydropower, and irrigation schemes [15]. Several treatments were used for the removal of WH. These are biological such as insects and fish, mechanical such as harvesting and chopping, and chemical methods. However, each of the methods was not effective [16]. Previous studies indicated that AC with a high specific surface area and highly porous surface that can remove any organic pollutant including dye can be achieved by processing hyacinth plants [17].

Several treatment methods have been adapted to remove dyes such as chemical methods (coagulation or flocculation with floatation and filtration), physical methods (membrane –filtration process, adsorption, reverse osmosis, and nanofiltration), and biological methods (aerobic and anaerobic methods) but have their limitation like sludge formation, waste disposal problem, high operation cost, and time-consuming [18]. Studies show that among many methods, an effective result was obtained from adsorption and photocatalysis [19].

Adsorption is a non-destructive process in which the transfer of solute takes place from one phase to another and is widely used for the removal of dye due to its high removal efficiency and simple operational cost. However, the essential regeneration process of AC is expensive and time-consuming [20]. Photocatalysis is on the other hand one of the advanced oxidation processes which generate highly reactive hydroxyl radicals and other strong oxidants, which are capable of mineralizing recalcitrant pollutants into harmless substances [21]. Titanium dioxide (TiO_2) is the most common photocatalyst that can be used for such purposes. This is due to its high activity, chemical stability, low cost, and superior photoactivity over other semiconductors that have been investigated [22]. TiO_2 has three different phases. These are anatase, rutile, and brookite. Each phase has different physical properties and physicochemical reactivity. The anatase phase exhibits higher photocatalytic activity than the two other phases and is mostly used for photocatalytic activity [23]. However, it is difficult to separate the photocatalyst, TiO_2, from water effluent after degradation and particles have the ability to agglomerate at a high concentration which decreases the photocatalytic efficiency [24]. Immobilization of TiO_2 on support material has been suggested to alleviate this problem. Previous studies show the immobilization of TiO_2 on fixed supports such as glass, fibers, quartz, and stainless steel [25].

However, the efficiency of photocatalysis regularly decreases on such immobilized TiO_2 catalysts because of limitations in mass transfer and toxic shock to the system. The main criteria for support materials are high specific surface area and porosity to allow immobilization, low density, and high adsorption capacity [26]. WHAC has a high specific surface area, porosity, and low density, which makes it suitable support for the synthesis of TiO_2/WHAcc. Another advantage of WHAC as support is the reduction of a toxic shock to the system by sufficient adsorption of contaminants and the ability to adsorb pollutants, and release them onto the surface of TiO_2.

In this study, the synthesis and characterization of TiO_2/WHAcc is investigated. The sol-gel method is employed to prepare the catalyst and the morphology of the as-prepared catalyst material is characterized using FE-SEM. Further, FT-IR spectroscopy, BET/BJH analyzer, and XRD are used to identify the functional groups, surface area, pore volume, and phases present in the catalyst. Finally, the samples are tested for the removal and degradation of MB dye from wastewater effluent. MB is used as the dye because it is found in most process effluents [27].

1.2 Statement of the problem

Most dyes and their intermediates have teratogenic, carcinogenic, mutagenic effects, and high biological toxicity. To date, several methods, physical, chemical, and biological methods, have been adopted for the removal of dyes. These methods have their limitations such as sludge formation, waste disposal problem, secondary pollution, high operation cost, and time consumption.

Studies show that effective removal of dyes can be achieved by employing adsorption and photocatalysis [28]. However, adsorption require a regeneration process that is expensive and time-consuming. The most widely used photocatalyst, TiO_2, has limitations such as difficulties in separating TiO_2 from water and high concentration of TiO_2 leads to agglomeration. As a result, the efficiency of TiO_2 photocatalyst can be reduced. Catalyst separation and high recovery cost are the main drawbacks in slurry type photoreactor because it needs nano-filtration which is very expensive and catalyst leachate can be a health and environmental concern.

WHB is widely spread in most lakes in Ethiopia mainly in the largest lake, Lake Tana. The plant profoundly changes the ecosystem that invades extremely and quickly by producing their daughter plant on stolon's 10 plants can produce a mat of 650,000 plants in one growing season and consumes a large number of minerals and blocks sunlight by suspending on the lake. It has been employed for AC production purposes and outstanding results of high surface area have been recorded. In addition, WHB is cheap and easily available making the hyacinth plant feasible for AC application and suitable for supporting the TiO_2 catalyst material due to high surface area, low density, high adsorption capacity, and reduction of toxic shock. A catalyst material can be synthesized from AC and TiO_2. TiO_2 catalyst immobilized AC can give higher photocatalytic properties and higher pollutant removal efficiencies.

1.3 Objectives of the Study

1.3.1 General Objective

The general objective of this study is to synthesize and characterize TiO_2 immobilized water hyacinth-based activated carbon catalyst for the removal of methylene blue dye.

1.3.2 Specific Objectives

The specific objectives of this study are:

- To develop activated carbon from WHB.
- To investigate the possibility of immobilizing TiO_2 on WHAC.
- To investigate the physicochemical characteristics of the as-synthesized catalyst material.
- To investigate the MB dye removal efficiency of WHAC and TiO_2/WHAcc.

1.4 Scope of the Study

This thesis work focuses on the characterization, photocatalytic degradation, and adsorption of MB using WHAC and TiO_2/WHAcc under ultraviolet (UV) irradiation.

1.5 Significance of the Study

Lake Tana is the biggest lake found in the northwestern part of Ethiopia. This lake has been facing several problems in its water volume and ecosystem due to the aggressively spreading WHB. The main approach to solve this problem is the hand removal of the plant from the lake. Literatures indicate that AC with a highly porous surface that can remove any organic pollutant can be achieved by processing the hyacinth plant. This work presents AC prepared from the hyacinth plant that will be combined with TiO_2 to make catalyst material that can be used for wastewater treatment. The porous surface of AC combined with TiO_2 will form a material with the advanced property. The significance of this research is that it starts from waste material from Lake Tana which is easily available and cost-effective. A synthesized catalyst material will be used for the degradation of MB dye which is a very toxic chemical discharged from the textile industry. Hence, the study contributes an alternative method for the removal of MB dye and to reduce the problem that occurs due to WHB in Lake Tana. Therefore, this study plays a significant role in environmental and socio-economic aspects.

CHAPTER TWO

2. LITERATURE REVIEW

2.1 Water Hyacinth

Water hyacinth (*Eichhornia Crassipes*) is an aquatic plant that can live and reproduce floating freely on the surface of fresh waters or can be anchored in muds. The plants are up to 1-meter height although 40 cm is the more usual height. The inflorescence bears 6-10 lily-like flowers, each 4-7 cm in diameter, from a few inches to a meter in height. Its rate of proliferation under certain circumstances is extremely rapid and it can spread to cause infestations over large areas of water causing a variety of problems. It grows in mats up to meters thick which can reduce light, oxygen, change water chemistry, and affect flora and fauna, and cause a significant increase in water loss due to evapotranspiration [29].

2.1.1 Characteristics of Water Hyacinth

WH has an excellent ability to take up nutrients and other chemicals from its environment and the chemical composition of the WH depends strongly on its environment. The nutrient content is lower in the stem and root compared with the nutrient content in leaves. Fresh WH plant contains 95.5% moisture, 0.04% N, 1.0% ash, 0.06% P_2O_5, 0.20% K_2O, and 3.5% organic matter. On a zero- moisture basis, 75.8% organic matter, 1.5% N, and 24.2% ash [30]. WH powders have a very high adsorption capacity for heavy metals (Cr, Cu, Ni, Pb, Zn), and tend to form a strong bond with direct dyes, reactive dye, azo dyes, basic dyes, and acidic dyes [31]. The ash contains 28.7% K_2O, 1.8% Na_2O, 12.8% CaO, 21.0% Cl, and 7.0% P_2O_5. The CP contains, per 100 g, 0.72 g methionine, 4.72 g phenylalanine, 4.32 g threonine, 5.34 g lysine, 4.32 g isoleucine, 0.27 g valine, and 7.2 g leucine [32]. Gohl reported that 5.9 g dry matter of Indian hyacinth contains 28.7% K_2O, 1.8% Na_2O, 12.8% CaO, 21.0% Cl_2, and 7.0% P_2O_5 [33]. Nutritive values showed that its 100 g crude contains 13.1% of crude proteins, 18.2% crude fibers,15.3% ash, and 2.16% Ca.

Table 2-1 Chemical analysis of dried WHB [34].

S. No.	Composite (%) Dried Weight	Leaves	Stems	Roots
1	Carbon	30.33	29.55	27.22
2	Nitrogen	0.3	0.2	0.1
3	Cellulose	29.86	29.33	18.11
4	Hemicellulose	31.81	28.35	15.67
5	Lignin	5.49	18.36	15.67
6	Protein	21.97	7.70	3.33
7	Lipid	1.93	0.98	0.65
8	Ash	13.10	21.20	50.11
9	Calorific value (KJ/g-DW)	15.33	14.55	9.5

2.1.2 Controlling Mechanisms of Water Hyacinth

There are several popular control mechanisms for preventing the spread of WH. The three main mechanisms used are biological, chemical, and physical controls. Each has its benefits and drawbacks [35].

2.1.2.1 Biological method

Biological control is the use of host-specific natural enemies to reduce the population density of a pest. Several insects and fungi have been identified as control agents for WH. Biological control of WH is said to be environmentally favored as the control agents tend to self-regulate themselves. The major drawbacks are insufficient reduction, and it can take several years for the insect population on density sufficient to tackle the pest problem [36].

2.1.2.2 Chemical method

The application of herbicides for controlling WH has been carried out for many years. The common herbicides are 2,4-D, diquat, and Glysophate. Herbicides application as a control method is usually less expensive than mechanical control, but it has to be accountable for human and ecosystem health. The main drawbacks of these methods are the lack of control of large infestations and long-term adverse effects on other communities and the environment [37].

2.1.2.3 Physical methods

Physical methods consist of two kinds of control: manual and mechanical removal. Manual removal is done by a human, to remove the WH plants from the water bodies, while the mechanical removal method is carried out by machines. Mechanical removal of WH consists of using weed cutters, harvesters, chaining, shredder boats, and dredging process. Mowing, netting, and barriers are also used as ways of mechanical removal [38]. Manual removal of WH is suitable only for extremely small areas because it requires labor-intensive work and in some areas, there are serious health risks associated with the work (crocodiles, hippopotamus, and bilharzia). Transportation of the harvested weed is so costly because of a high-water content. Besides these three mainstream forms of control, Harley et al. suggested another method namely the reduction of nutrients inputs to the water [39]. In recent decades, there has been a significant increase in the level of nutrients dumped into waterways from industrial and domestic sources as well as from land where fertilizers are used.

2.2 Titanium (IV) Dioxide

Titanium dioxide (TiO_2), also called titanium (IV) oxide or titanium, was discovered in 1791. Impure titanium was prepared by Nilson and Pettersson in 1887; however, the pure metal (99.9%) was not made until 1910 when Hunter heated $TiCl_4$ with sodium in a steel bomb [40]. Among the other semiconductors, TiO_2 has become a promising material that has been widely used in photocatalytic processes due to its superior properties, such as excellent optical and electronic properties, high photocatalytic activity, high chemical stability, low cost, non-toxicity, and environmental friendliness [41].

2.2.1 Fundamental Properties of Titanium Dioxide

TiO_2 products are white powders and have three crystalline structures: anatase, rutile, and brookite. Rutile is the most thermodynamically stable crystalline structure of TiO_2 but anatase is the preferred form for photocatalysis since it presents higher photocatalytic activity.

The anatase phase has high photocatalytic property due to the greater hole trapping ability which shows a lower recombination rate compared to the rutile phase. Anatase crystal structure is found to be a common candidate for catalyst modification for its stable configuration suitable for photodegradation studies Therefore, anatase is considered the most photochemical active phase of TiO_2 due to the aforesaid combined properties [42]. Brookite is a metastable phase. Brookite is often observed as a by-product when the precipitation is carried out in acidic and pure brookite without rutile or anatase is rather difficult to be prepared so that, until recently, its photocatalytic properties have been not much studied [43].

2.2.2 Photocatalytic Application of Titanium Dioxide

TiO_2 is considered a good semiconductor. It absorbs electromagnetic radiation in the near UV region. The difference in energy between the valance band and conduction band in the solid states is 3.05 eV for rutile and 3.29 eV for anatase, corresponding to an absorption band < 415 nm for rutile and < 385 nm for anatase. The first step for the occurrence of photodegradation by semiconductor photocatalyst is the absorption of light energy to promote electrons from the valance band to the conduction band. These electrons and similarly created holes can move on the surface of the solid and a redox reaction takes place [44]. Due to the non-biodegradability nature of synthesized dyes, conventional biological treatment processes are ineffective. Adsorption and coagulation practices result in secondary pollution. Consequently, a more promising technology based on advanced oxidation processes has been studied extensively for decolorization and degradation of textile dyes. The photocatalytic decolorization of a dye takes place according to the following mechanism. When a catalyst is exposed to UV radiation, electrons are promoted from the valance band to the conduction band and an electron-hole pair is produced. For example, water molecules that are adsorbed on the surface of TiO_2 catalyst will be oxidized at the surface producing hydroxyl radicals. The hydroxyl radicals are a highly stronger oxidizing agent than either ozone or chlorine, both known as stronger oxidants.

There are different materials used as a photocatalyst of which TiO_2 is considered as the best photocatalyst. The primary reason for an efficient semiconductor photocatalyst is the redox potential of the charge couple, electron-hole pairs lie within the bandgap domain of the photocatalyst. In addition to possessing suitable bandgap energy, an ideal semiconductor should also be easy to produce (cost-efficient), photo-stable, and non-harmful for humans and the environment [45]. Among all the photocatalysts studied so far, titanium dioxide (TiO_2) has emerged as a leading photocatalyst for environment purifications due to its strong oxidizing

power under ultraviolet irradiation, high chemical stability, low cost, and environment friendly [46]. Anatase is considered the most photochemical active phase of TiO_2 [47].

2.2.3 Photocatalytic Mechanism of Titanium Dioxide

TiO_2 in the anatase and rutile phase has different bandgaps. When the energy of a photon from the light source exceeds this gap, < 388nm, a photo-excited electron will be promoted to the conduction band, leaving a positive hole in the valance band, this is called the electron-hole pair (e-, h+). The charged particles can recombine to produce heat, become trapped, or migrate to the surface to participate in a series of redox reactions. During UV irradiation into an aqueous solution for degradation, the catalyst remains in an electronic equilibrium, where at a steady-state there is an equal rate of electron and hole migration to the surface[48]. Surface trapped holes are responsible for the mineralization of organic micro-pollutants by either direct oxidation between the pollutant and hole or by reacting with surface adsorbed molecular water and hydroxide ions to produce hydroxyl radicals. As the holes are involved in the oxidation reaction, the surface electron must also react to maintain the charge equilibrium and minimize recombination. Oxygen is used as an electron scavenger due to the minimal processing cost of sparing the solution with air. Dissolved oxygen will adsorb onto the catalyst surface and be reduced by the surface trapped electron. Even though hydrogen peroxide is produced, its contribution to the reactive hydroxyl radicals toward mineralization is deemed minimal.

TiO_2 has been used as an effective catalyst for photobleaching or photodegradation of many structural classes of organic dyes in an aqueous solution, using UV light. However, the result from a study of 15 dyes indicates that photobleaching rate differs significantly from a family of dyes with different functionalities and depends on the light source and crystallinity of the titanium dioxide used. The average bleaching rate of anionic dyes are faster than cationic dyes and, neutral dyes were the slowest to be bleached using titanium dioxide and visible light photocatalyst .

Among all semiconductor photocatalysts, TiO_2 is receiving a higher concern as a promising photocatalyst due to its superior characteristics, such as nontoxicity, chemical stability, highly photo-catalytic activity, ability to be coated as a thin film on a substrate, environmentally friendly [49].

Currently, TiO_2 NPs are produced abundantly and used widely because of their high stability, anticorrosive, photocatalytic property, photostability, ease of availability, bio-inertness, low energy consumption, low operational temperature, relatively high chemical stability, suitable flat band potential, etc. [50]. However, the application of TiO_2 for the treatment of wastewater on an industrial viable scale continues to face a series of technical challenges. One issue that hinders the application of TiO_2 on an industrial scale is the fine part size of TiO_2, combined with its large surface area to volume ratio and high surface energy, which makes it inclined to agglomeration and difficult to decant [51].

2.3 Activated Carbon

AC, also widely known as activated charcoal or activated coal is a form of carbon that has been proposed to make it extremely porous and thus to have a very large surface area available for adsorption or chemical reactions [52]. Due to such a high degree of porosity, just one gram of AC has a surface area above 500 m^2 (about one-tenth the size of an American football field), as typically determined by nitrogen gas adsorption sufficient activation for useful applications may come solely from the high surface area, though further chemical treatments which generally enhance the adsorbing properties of the material [53].

2.3.1 Preparation of Activated Carbon

AC is produced from carbonaceous materials such as nutshells, peat, wood, coir, lignite coal, and petroleum pitch. It can be produced by physical activation or chemical activation methods.

2.3.1.1 Physical activation

Physical activation is a two-step process. It involves the carbonization of raw materials followed by activation at elevated temperatures ranges between 800−1100 °C. Generally, CO_2 is used as an activation gas and CO_2 activation process is cleaner, easy to handle, and easy to control the activation process due to the slow reaction at high temperature ranges between 800−1100 °C [54].

2.3.1.2 Carbonization

The method of production of carbonized intermediates products has a marked effect on the quality of the final AC products. The main aim of carbonization is to reduce the volatile content of the source material to convert it to a suitable form for activation. During the phase of carbonization, the carbon contents of the product attain a value of about 80 percent, and most of the non-carbon elements, hydrogen, and oxygen are first removed in gaseous form by pyrolytic decomposition of the starting material and the free atoms of elementary carbon are grouped into an organized

crystallographic formation known as elementary graphitic crystallites. The carbonization of lignocellulosic materials starts above 170 °C and it is nearly completed around 500-600 °C [55]. In the production of charcoal, it is desirable to carry out the pyrolysis sufficiently and quickly to reduce the time for the formation of carbon. The rate of pyrolysis is significantly influenced by the moisture content of the starting material. Further important factors are uniform heating of the retort and the temperature of carbonization which must not be very high. In the simple carbonization product, the mutual arrangement of the crystallites is irregular so that free interstices remain between them. However, as a result of deposition and decomposition of tarry substances, these become filled or at least blocked by disorganized (amorphous) carbon. The resulting carbonized products have a small adsorption capacity. Presumably, at least for carbonization at lower temperatures, part of the formed tar remains in the pores between the crystallite and on their surface. Such carbonized materials can be partially activated by heating them in a stream of inert gas, or by extracting them with a suitable solvent or by a chemical reaction.

During heating in an inert atmosphere, the molecular bond of cellulosic materials will be broken. Since C-O bonds are weaker than the C-C bonds, the principal candidates for scission are the 1,4 C-O-C glucosides and the 1,5 C-O-C acetyl linkages in the cellulose macromolecules. The breakages of 1,4 glycoside bonds result in de-polymerization of cellulose and are responsible for the formation of tars. The breakage of 1,5 acetyl bonds leads to ring-opening and results in the formation of gases and chars.

2.3.1.3 Activation with gaseous agents

A carbon with a large adsorption capacity can be produced by activating the carbonized material under such conditions that the activating agent reacts with the carbon. The most common activating agents are steam, carbon dioxide, and oxygen (air). The activation step is generally conducted at a temperature between 800- 1100 °C. The active oxygen in the activating agent burns away the more reactive portion of the carbon skeleton as carbon monoxide and carbon dioxide, depending on the gaseous agent employed. The reaction of carbon with carbon dioxide is endothermic and, for a given carbon in the absence of a catalyst, takes place at a rate several orders of magnitude slower than the carbon-oxygen reaction at the same temperature. It proceeds very slowly at temperatures below 1000 K (727 °C).

During the precursor carbonization, volatile matter, aliphatic carbons, and heteroatoms are released, while residual carbon atoms are grouped into stacks of flat aromatic sheets cross linked randomly. The irregular arrangement of these carbon sheets gives rise to free interstices that correspond to an incipient porosity, which can be further developed by the gasification that takes place during physical activation. Further, new pores can be created and material that eventually was blocking the entrance of existing pores is removed. As a result, a pronounced increase of the available porosity and surface area takes place [56].

2.3.1.4 Chemical activation

During the preparation of activated carbon, physical activation, chemical activation and physical−chemical activation are very common. Compared with the physical activation method at relatively high temperature the chemical activation method at a comfortable temperature has higher activated carbon yield, less environmental pollution, and is widely used. Chemical activation is done by impregnating the material with an activator and then performing a heat treatment between 400 and 900 °C, where the process of preparing activated carbon is carbonized and activated simultaneously. Activators are crucial impactors in chemical activations. H_3PO_4 was usually used as the activator for promoting bond cleavage reactions and protecting the internal pore structure at the same time in chemical activation [57].

Moreover, the yields of carbon in chemical activation are usually higher than those in physical activation because the chemical agents used are substances with dehydrogenation properties that inhibit the formation of tar and reduce the production of other volatile products.

On calcinations, the impregnated chemicals, dehydrate the raw materials, which results in changing and aromatization of the carbon skeleton by the creation of porous structure and high surface area. The materials mainly used in the production of AC consist predominantly of cellulose, and therefore in the discussion of the mechanism of chemical activation, the action of chemical agents of cellulose must first be considered. Cellulose is composed of elongated macromolecules, up to 1800-2000 nm long, oriented in the direction of their longitudinal axes, which form agglomerates known as micelles. The oriented chains of molecules are laterally bounded by bonds of different types of strength. The electrolytic action of the activation agent causes the cellulose to undergo a change known as swelling, during which the arrangement of the molecule in the direction of the longitudinal axis remains unchanged, but the lateral bond is broken down with the result that the intra and inter cell voids increase until finally the cellulose is dispersed. Simultaneously other reactions, hydrolytic or oxidative, takes place, by which the macromolecules are gradually depolymerized. The process leads to the formation of a homogenous plastic mass consisting of the partially depolymerized substance uniformly saturated with the activation agent. Several dehydration agents such as KOH, NaOH, H_3PO_4, $ZnCl_2$, Na_3PO_4, NaCl, and $KMnO_4$ were used on various raw materials to yield appreciable quality of AC. The ACs produced through chemical activation especially when $ZnCl_2$ is used must be cleaned from the chemical agent before their commercial use. One advantage of using H_3PO_4 in chemical activation is that can be cleaned from the AC by rinsing with boiling pure water [58].

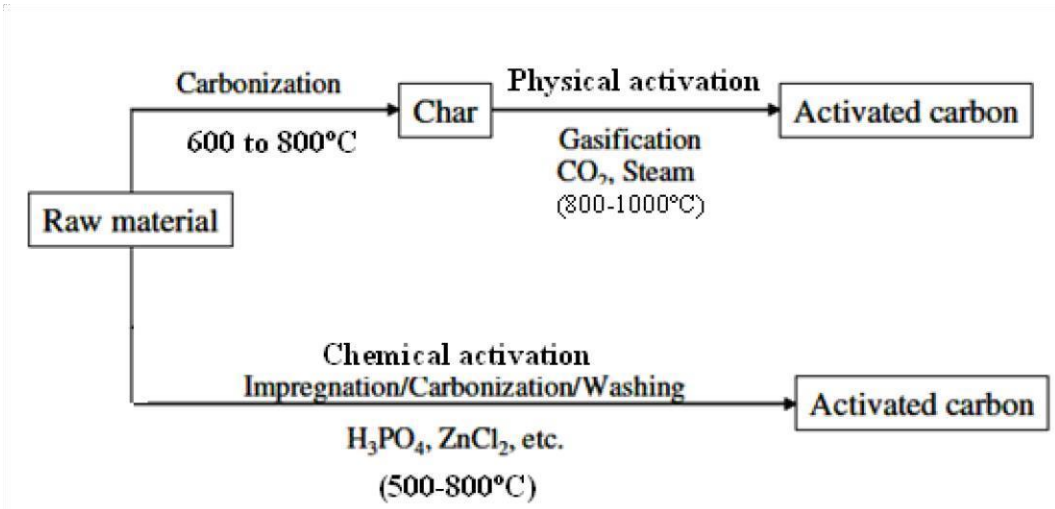

Figure 2-1 Flow diagram for the production of activated carbon.

Generally, activation with phosphoric acid is commonly used for lignocellulosic material and at lower temperatures [59]. The influence of the experimental conditions such as temperature, heating rate, and residence time can be interpreted in terms of competition between two types of cellulose degradation. Lignocellulosic biomass is widely used for biochar production, which has been often carried out at a wide range of temperatures from 200 to 1200 °C. Increasing the pyrolysis temperature at peak level during pyrolysis, creates a negative impact on the biochar yield because the high temperature facilitates the thermal cracking of biomass.The pyrolysis characteristics of lignocellulosic components, such as hemicellulose, cellulose, and lignin have already been well investigated [60].

2.4 Synthetic Dyes

Dyes are a type of organic compound that can provide bright and lasting colors to other substances. Currently, there are about 100,000 different commercial dyes and pigments and over 7×10^5 tons of synthetic dyes are produced annually worldwide, which are specifically designed to resist fading upon exposure to sweat, light, water, and oxidizing agents, very stable and difficult to degrade. Synthetic dyes have been increasingly used in the textile, leather, paper, rubber, plastics, exist structures that make them more stable and less biodegradable.

The major components of dye molecules are chromospheres and auxochromes. A chemical structure, which is colored is normally accomplished in the synthesis of dyes using chromospheres with an autochrome. The chromosphere group is a color give, which forms a basis for the chemical classification of dyes when coupled with chromogenic. Most chromospheres are azo (-N=N-), carbonyl (-C=O), and nitro ($-NO_2$) groups. The chromogen, which is the aromatic structure normally contains benzene, naphthalene, or anthracene rings, is part of a chromogen-chromophore structure along with an auxachrome. The presence of an ionizing groups known as auxachromes results in a much stronger alteration of the maximum absorption of the compound and provides a bonding affinity [61].

Dyes can be classified in many ways. “The organic chemists classify them according to their common parent structure (Chemical Classification). The dyer, who is only interested in fixing the dye to the fiber, classifies them according to their method of application”. Dyes used in textile industries are classified into three classes: (a) anionic (direct, acid, and reactive dyes), (b) cationic (all basic dyes), and (c) nonionic (dispersed dyes) [62].

Textile dyes have been classified according to their chemical structure (Azo dyes, Nitro dyes, Indigo dyes, Anthraquinone dyes, Phthalein dyes, Triphenyl methyl dyes, Nitrated dyes, etc.) or their industrial application [63]. According to Lucas et al., and other have been reported to Azo dyes are the largest class of synthetic dyes. Approximately 70% of all the dyes used in industry are azo dyes. They are widely used in textile, cosmetic, leather, pharmaceutical, paper, paint and food industries [64].

2.5 Color Removal Method from Textile Wastewater

Textile organic dyes must be separated and from water streams especially from industrial wastewaters by effective and viable treatments at sewage treatment works or onsite following two different treatment concepts; by separation of organic pollutants from water environment or by partial or complete mineralization or decomposition of organic pollutants. The separation process can be based on sedimentation, centrifugation, filtration, and floatation or synthetic membranes (nano filtration and reverse osmosis). Additionally, physicochemical precipitation, coagulation-flocculation, and ionic exchange can be used to separate discolored, emulsified, and solid compounds from the water environment [65]. The conventional methods for the treatment of colored wastewater are physical, chemical, and biological treatments. These technologies have their own advantages and disadvantages [66].

2.5.1 Physical Methods

Physical dye removal methods are methods usually accomplished by mass transfer method. This method includes filtration process, reverse osmosis, electrolysis and adsorption techniques. The major drawback in this technology, especially membrane filtration is limited life time before membrane fouling occurs and as such the cost of periodic replacement must thus be included in any analysis of their economic viability. Among all the physical treatments, adsorption process has been reported to be the most effective method for water decontamination [67].

2.5.2 Chemical Methods

Chemical methods include coagulation or flocculation combined with floatation and filtration, precipitation, electro floatation, electro kinetic coagulation, conventional oxidation methods by oxidizing agents such as ozone, irradiation or electrochemical processes. Though the dyes are removed completely by this process, it is so expensive and also accumulation of concentrated sludge creates a disposal problem [68].

2.5.3 Biological Methods

Biological methods, i.e. degradation of dyes with the biological phenomenon such as

bioremediation is a green technique to remove dye from textile effluent with minimum cost and optimum operating time. The biological degradation (i.e., bioremediation) is economically feasible, environmental-friendly and generates less volume of sludge when compared with other techniques. It causes the degradation of synthetic dyes to a comparatively less toxic inorganic compound because of the breakdown of bond (i.e., chromophoric group) and finally helps in the removal of color. [69].

2.6 Adsorption

One of the most effective and proven treatments with potential applications in textile effluent treatment is adsorption. This process consists of the transfer of soluble organic dyes (solutes) from wastewater to the surface of solid (the adsorbents) with high porosity. The adsorbent has a finite capacity for each compound to be removed.

Adsorption is an economically feasible process for dye removal. The decolorization of textile effluents is the result of the adsorption and ion exchange mechanisms. The principal influencing factors in dye adsorption are adsorbent surface area, particle size, temperature, pH, and contact time.

2.7 Titanium Dioxide/Activated Carbon Composite

Bestani et al. impregnated anatase TiO_2 into grape marc-based activated carbon (GMAC) particles. The TiO_2/GMAC was prepared by the original approach of the impregnation process using a chemical agent. The composite acting a photocatalyst has been used for the removal of reactive black 5 dye (RB5) from an aqueous solution. The surface area of TiO_2/GMAC, GMAC, and Anatase-TiO_2 was 1168, 914, and 117 m^2 g^{-1}, respectively. The hybrid photocatalyst shows better photocatalyst performance than both TiO_2 and GMAC [70].

Bahram et al. immobilized TiO_2 nanoparticles on a porous and low-density granular activated carbon (GAC) support for photocatalytic degradation of furfural. The TiO_2/GAC composite was synthesized using a simple sol-gel method. The effect of operational parameters of furfural concentration (200-700 mg L^{-1}), initial pH (2-12), catalyst dosage (1-3.5 g), and irradiation time (20-120 min) were studied. The synthesized TiO_2/GAC composite exhibited a total pore volume of 0.13 cm^3 g^{-1} and a specific surface area of 35.91 m^2 g^{-1}. Highest removal efficiency up to 95% was achieved at an initial pH of 10, catalyst dosage of 2.5 g, and irradiation time of 80 min. The photocatalytic TiO_2/GAC could be reused at least for four consecutive times with only a 2% decrease in furfural removal efficiency [71].

Corina et al. prepared AC from Sterculia foetida, TiO_2, and their composite for dye removal. The mixture of AC (activated at 600 °C) and titanium (calcined at 500 °C) has an impregnation ratio of 1:1. The composite showed higher removal efficiency than individual components [72].

Commonly applied methods for the synthesis of catalysts include molecular designed dispersion, sol-gel method. The sol-gel method of metal alkoxides involves two main reaction types: hydrolysis and condensation [73]. Conventional slurry impregnation or solvent assisted spreading [74], (either sequential and/or simultaneous wet impregnation [75], equilibrium deposition Filtration (EDF), The equilibrium deposition filtration (EDF) method, an advanced catalyst synthesis route that is based on a molecular level approach, can be used for tailoring the oxometallic phase deposited on a porous oxide support [76], sequential and simultaneous incipient wetness (pore filling) impregnation [77]. Since the incipient wetness impregnation

method is widely used in the industry for its simplicity and most of all because it allows saving on the energy-consuming step of the elimination of a large amount of water, this method will be applied in this study. However, the final dispersion of the active phase is negatively affected by the calcination step [78]. The preparation procedure of this technique involves impregnation, drying, calcination, and activation.

The most important step is the impregnation of the support particles or pellets with an aqueous solution containing species of the active and/or promoter ions. The impregnation step influences the structure and the dispersion of the active phase [79]. There are also different methods to synthesize metal oxide-supported catalysts. These are the sol-gel method, hydrothermal method, emulsion (micelles) techniques, chemical vapor deposition method, flame spray process. Impregnation is a method in which a certain volume of solution containing the precursor of the active phase is contacted with the solid (support or another active solid phase), which, in a subsequent step, is dried to remove the imbibed solvent [80].

Two most commonly used impregnation methods are distinguished, namely, wet (non-dry) impregnation (WI), whereby an excess amount of solution is used, and pore volume impregnation (PVI), in which an amount to just fill the pore volume of the support is used. The latter method is also known as incipient wetness impregnation (IWI) or dry impregnation (DI) because the impregnated material keeps a dry character at a macroscopic scale. In WI, the impregnated support is filtered out, leaving excess liquid containing any precursor that was not retained by the support. This entails a need to recycle the excess liquid to minimize wastage of the precursor. The use of DI eliminates excess liquid and the need for a filtration step. Common precursors include inorganic metal salts, such as metal sulfates, carbonates, chlorides, nitrates, or acetates, and organic metal complexes, such as metal acetyl acetones. The most commonly used solvent for inorganic salts is water because of the high solubility of many precursors, whereas organic solvents are mainly used for organometallic precursors [81].

Table 2-2 Comparison of dye removal methods [82].

Dye Removal Methods	Main Characteristics	Advantages	Disadvantages
Chemical precipitation	Uptake of the pollutants and separate the product formed	Use simple equipment, very efficient for metals and fluoride elimination, significantly reduce chemical oxygen demand	High sludge production, chemical consumption (lime, oxidants, H_2S)
Advanced oxidation process (AOP) Homogenous and heterogeneous photocatalytic process	Destructive technique	No production of sludge, rapid degradation, efficiency for non-biodegradable chemicals (dyes, drugs)	
Coagulation/flocculation	Uptake the pollutants and separate the product formed	Good sludge settling, the initial capital cost is cheap	Increase sludge volume generation, cause disease to human being like Alzheimer's, a neurotoxin, carcinogen caused by inorganic salts
Flotation	Separation process	Efficient for the removal of small particles and can remove low-density particles which would require low settling	High initial capital cost, selectivity is pH-dependent

treatment, hydrogen peroxide)	Use of biological (pure or mixed culture)	Simple, economical, and accepted by the public	Necessary to create an optimum favorable environment, slow process, low biodegradability High energy, maintenance, cost requirement, the choice of membrane depend on the specific application Rapid saturation and clogging of the reactors (regeneration is an expensive and time-consuming process) Expensive costs for a high volume of water (energy consumption, the volume of the concentrate and cost of the disposal
Biological methods (aerobic small space, rapid and	Nondestructive and anaerobic process)	It requires	
separation	efficient process, no chemical requirement)		
Membrane filtration (microfiltration, ultrafiltration,	Nondestructive	Nano filtration) Simple equipment, highly	
effective	process, use of a process (adsorption) with fast kinetics solid material		
Adsorption (commercial activated carbon (CAC), commercial activated alumina			
Concentration	Several types of evaporators exist on		
	technique		
(CAA), and mixed materials) for cyanide and		the market Efficient process sulfide	
removal life(ozone), the release of volatile		Evaporation	
$KMnO_4$) compounds			

CHAPTER THREE

3. MATERIALS AND METHODS

3.1 Materials

In this research work, raw materials of different chemicals, which were utilized for the synthesis of WHAC and TiO_2/WHAcc are H_3PO_4 (Loba Chem, 85 %), titanium butoxide (Ti $(OC_4H_9)_4$), (Cica-Reagent, 97 %), nitric acid (HNO_3) (Loba Chem, 71 %), and methylene blue powder (MB) (UNI-CHEM). Additionally, distilled water and ethanol were used for all the synthesis and treatment processes as a solvent for dissolving chemicals and for washing purposes during vacuum filtration and centrifugation.

Cross beater mill was used to perform size reduction and particle size distribution was made using a sieve analysis. Soaking and mixing were conducted using different sized borosilicate glass beakers and volumetric flask. An electronic balance was used to weigh samples. Subsequent sample drying and moisture removal were performed using a digital electronic oven. pH meter (Schott AG, Mainz, Germany) was used to adjust the acidity. An orbital shaker (EXCELLA E24R) was used to mix the adsorbate with water. A moisture analyzer (OHAU, Germany) was used to measure the moisture of raw WHB. During TiO_2/WHAcc and WHAC washing, separation of liquid and solid was performed by centrifuge and vacuum filtration using (filter paper), respectively. Nabertherm GmbH furnace equipped with digital display (bahnhofstr.20, 28865 Lilienthal/Bremen, Germany) was used to carbonize the WHS and calcination of the catalyst. The morphological structures and elemental distribution of the produced WHAC and TiO_2/WHAcc were analyzed using FE-SEM equipped with EDX. The phase, functional group, and surface area analysis were studied using XRD, FTIR, and BET-BJH method, respectively. Adsorption and photocatalytic experiments were performed by using conical flasks through magnetic stirrer, microbial hood, and UV-spectrophotometer to determine MB absorbance.

3.2 Methods

3.2.1 Sample Preparation

WHB was collected from Lake Tana, which is found in the north-western part of Ethiopia. The collected WHB sample was first washed with tap water subsequently with distilled water for the removal of mud and dust particles that may have been presented on the surface. Then, it was chopped, and using the moisture analyzer, the content of moisture was determined to fix the drying temperature. The moisture content of raw WHB was 74.21 % and subsequently, oven-dried for 48 hrs. at 120 °C. The dried WHB was grounded to a fine powder using a cross beater mill and sieved to get a uniform size distribution between (1-2 mm). Proximate analysis (fixed carbon, volatile matter, ash, and moisture content) was analyzed. Finally, it was packed in a plastic bottle and used as a raw material throughout the experiment.

3.2.2 AC Preparation

The sieved sample was then impregnated with a solution of H_3PO_4 (25, 35, and 45%) with an impregnation ratio of 4:1 (w/w H_3PO_4 / WHB) [83]. The slurry was stirred with a magnetic stirrer for 4 hrs. and simultaneously heated at a temperature of 85 ℃ while stirring to facilitate the impregnation and dried in an oven at 105 ℃ for 24 hrs. The dried impregnated samples were put into porcelain crucibles and carbonized in a furnace (Nabertherm GmbH) at different carbonization temperatures of 400, 600, and 800 ℃ for 2 hrs. [84]. Then, carbonized materials were immediately taken into a desiccator to prevent contact with oxygen (moisture sacking) and allowed to be cooled to room temperature. Then the weight losses during carbonization were determined and recorded as yield. After the activation and carbonization step, the obtained AC was washed with distilled water until neutral pH was achieved. Lastly, AC samples were dried in an oven at 105 °C for 24 hrs. [85]. The samples were ground in an agate mortar and pestle to have an average diameter of 0.5 mm (20-50 mesh ASTM standard) [86] and packed in a plastic bottle for further use.

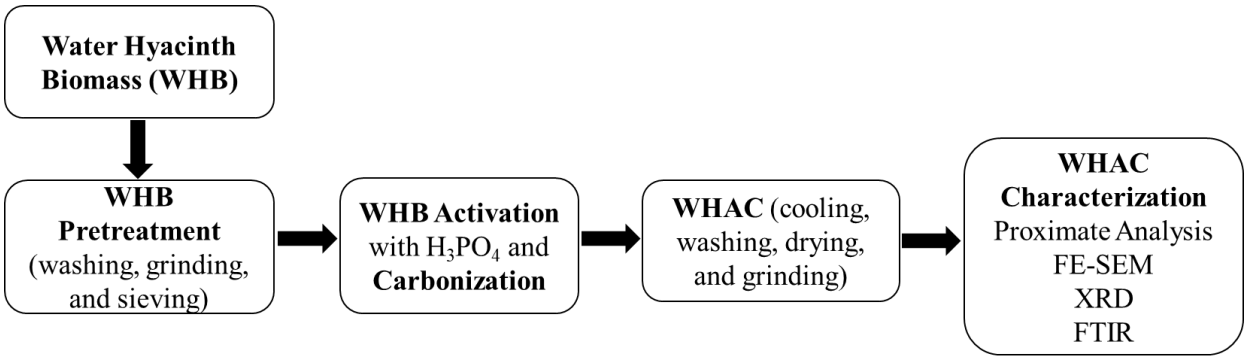

Figure 3-1 Steps involved in the production and characterization of WHAC

3.2.3 Synthesis of TiO_2 Impregnated WHAC Catalyst

The TiO_2/WHAcc was synthesized with the help of sol-gel method using titanium butoxide ($Ti(OC_4H_9)_4$ with a purity of 97 %) as a precursor. For the synthesis, 25 ml of $Ti(OC_4H_9)_4$ was dissolved in 50 ml ethanol and vigorously stirred until fully mixed using a magnetic stirrer (2500 rpm, IKARCT basic stirrer) at room temperature. Ethanol was used as a solvent to form TiO_2 precipitate. For hydrolysis of the solution, HNO_3 was added dropwise to adjust pH of 2.5 and 50 ml deionized water was also added dropwise under vigorous stirring for 1 hr. Then, 3 g WHAC was added and the mixture was stirred slowly at 500 rpm for 4, 8, and 12 hrs. After continuous stirring, the prepared samples were filtered using a centrifuge at 5000 rpm for 45 min and washed with ethanol and distilled water to remove impurities. The samples were dried using a digital electronic oven at 110 ℃ for 4 hrs. to remove the moisture. Finally, calcination of the as-prepared catalyst was performed to get TiO_2 impregnated AC using a furnace at 500 ℃ for 3 hrs.

3.3 Characterization of WHAC and TiO_2 Immobilized on WHAC Catalyst

3.3.1 Proximate analysis

Moisture content, ash content, volatile matter, bulk density, and fixed carbon content were determined according to ASTM, as presented in Table 3-1 (see Appendix A for detailed information).

Table 3-1 proximate analysis of WHB [87]

Proximate Analysis	ASTM
Moisture content	D4442-07
Ash content	E1755-01
Volatile matter	D3175-11
Fixed carbon	By weight difference

3.3.2 BET-BJH Analysis

The surface area and pore size distribution of the WHAC and TiO_2/WHAcc using the BET-BJH analyzer. The specific surface area and pore size distribution were determined by nitrogen adsorption-desorption at 77 K, outgas temperature and time was 300 °C and 16 hrs. respectively. The relative pressure (P/Po) was in the range of 0.1-1. The time required for each point of adsorption/desorption to attain equilibrium was 60/60 sec. The pore size distribution was analyzed by BJH method.

3.3.3 XRD Analysis

The crystalline phases were determined using DW-XRD-Y7000 instrument with Cu-Kα radiation (λ=0.15406), accelerating maximum voltage (40 kV), the current intensity of (30 mA), scan speed of 3 degrees per minute in the range of 2θ = 5-85°, and sampling pitch 0.0200 (deg). The crystallinity of the samples was determined based on the observed peak. The degree of crystallinity was taken as the ratio of the sum of areas under the crystalline diffraction peaks according to equation 3.2. Origin Pro (9.1 2019b) version was used to analyze and fit the observed peaks. The crystallite sizes of the lattice planes were estimated by using the well-known Scherer equation (equation 3.3).

The sample that was selected for XRD analysis was WHAC (600°C with 45% concentration) and TiO_2/WHAcc impregnated for (12 hrs.) because among the experiments best removal efficiency occurred on these samples.

$$\text{Crystallinity} = \frac{\text{Area of Crystalline Peaks}}{\text{Total area of peaks}} * 100 \quad \text{..... (3.2)}$$

where, D is average crystallite size (nm), k is constant (shape factor, about 0.9), β is the full width at half maximum (FWHM, in radian) and θ is peak position obtained from the XRD plot.

$$D = \frac{K\lambda}{\beta\cos\theta} * 100 \quad \text{..... (3.3)}$$

3.3.4 FT-IR Analysis

The functional group of WHAC (600 °C with 45 % concentration) and TiO_2 /WHAcc impregnated for (12 hrs.) was determined by Spectrum 65FTIR (PerkinElmer) in the range 4000-400 cm^{-1} using KBr pellet. Different types of chemical bonds and functional groups on the surface of the material and the chemical bonds in a molecule can be determined based on the respective functional group frequency range.

3.3.5 FE-SEM and EDX Analysis

The surface morphology of WHAC and TiO_2/WHAcc were analyzed using FE-SEM equipped with EDX. The FE-SEM images of the WHAC were obtained at different resolutions for different accelerating voltages. EDX technique was used for the elemental analysis or chemical characterization of a sample in conjunction with FE-SEM [88]. Gold is commonly used for the preparation of electron microscope specimens because of its high electrical conductivity and fine grain size resulting in high-resolution images. Thus, before the analysis, the samples were coated with gold to make them electrically conductive.

3.4 Adsorption

Adsorptive properties of adsorbent material were analyzed using conducting a batch adsorption experiment using standard MB ($C_{16}H_{18}ClN_3S$, AR grade) solution as a test dye molecule. To investigate the effect of relevant parameters, adsorption experiments were conducted in a batch test. 100 ml of MB dye solution of desired concentration (5, 7.5, 10, 12.5, and 15 mg L^{-1}) was prepared in a 250 ml conical flask by suitable dilution of the stock solution . Then, a known

amount of AC was added and the resulting mixture was stirred using a magnetic stirrer for a predefined time. After stirring, the suspension was decanted and the supernatant was analyzed for the dye removal percentage using UV-spectroscopy at 664 nm [89]. The final concentration of MB at equilibrium was measured from the calibration curve. To compare the extent of MB uptake by the different adsorbents, percentage removal was calculated once the equilibrium was achieved (C_e; mg L^{-1}) using equation 3.4.

$$\text{Percentage Removal} = \frac{Co - Ce}{Co} * 100 \quad \text{(3.4)}$$

where C_o (mg L^{-1}) is the initial concentration of MB and C_e is the concentration of MB at equilibrium.

The photocatalytic activity of the sample was evaluated by the degradation of MB in an aqueous solution. MB was used as a model pollutant and UV–visible spectroscopy was used to monitor the degradation under different conditions such as MB concentration, catalyst dose, and contact time. First, the MB solution at different concentrations (10, 15, and 20 mg L^{-1}) was prepared by dissolving the required quantity of the dye without further purification in distilled water [90]. Consequently, absorbance of the dye solution was measured by UV-spectroscopy and a linear absorbance versus concentration standard curve of MB was prepared. After the standard curve was plotted, the efficient catalyst was selected based on its dye removal efficiency among many

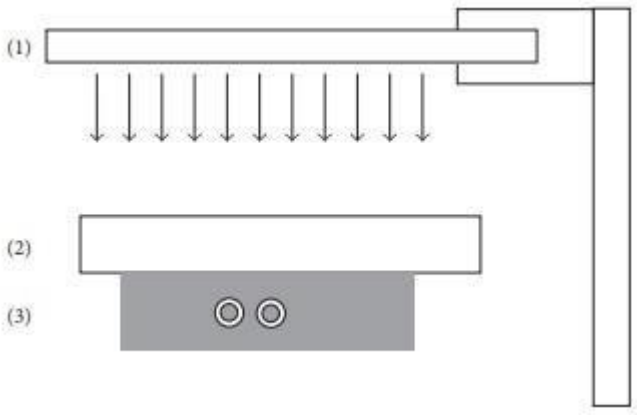

catalysts that were synthesized at different impregnation times.

Figure 3-2 Schematic of fludized bed photoreactor. (Adjustable UVC lamp, (2) Rectangular cubic reactor, and (3) Magnetic stirrer [91].

The absorbance of the samples was measured using a UV spectrophotometer at a maximum wavelength of 664 nm and the final dye concentration after treatment was determined from the absorbance and dye concentration standard curve. The dye removal efficiency was determined using equation 3.5.

$$\text{MB Removal (\%)} = \frac{Co - Ct}{Co} * 100 \quad \text{..... (3.5)}$$

Where, Co is the initial concentration of dyes in (mgL^{-1}) and; Ct is the final dye concentration in ($mgL^{-1)}$ after treatment is completed.

3.6 Experimental Design

RSM and BBD with three factors were used for experimental data analysis of MB removal efficiency using Design-expert 7.0 software. The results obtained from the experiment were analyzed with ANOVA to model the relationship between various factors and responses. The three variables studied for the removal of MB were catalyst dose, contact time, and dye concentration as summarized in table 3.2 whereas the response variable was MB removal efficiency.

Table 3-2 Independent variables and levels for BBD.

Factors	**Factor levels**		
	Low (-1)	Medium (0)	High (+1)
Catalyst dose (g)	0.05	0.1	0.15
Contact time (min.)	15	30	45
Dye concentration (mg L^{-1})	10	15	20

3.7 Selection of WHAC

To select the adsorbent 0.1 g WHAC that was prepared at different temperatures (400, 600, and 800 °C) and concentrations (45, 35, and 25 %) and 100 ml adsorbate was used from a dye concentration of 10 mg L^{-1} MB solution. Then a magnetic stirrer was used to mix the adsorbent with adsorbate with contact time for 30 min. After, that the decanted adsorbate was taken to a cuvette, and their absorbance was measured using UV-spectrometer.

3.8 Catalyst Selection

Among different catalysts synthesized at various impregnation times, the efficient catalyst was selected based on its dye removal efficiency. So, in this experiment, 0.1g of adsorbent with 100 ml adsorbate was used from a dye concentration of 20 mg L^{-1}, and a contact time of 15 min was used to select the best catalyst from (4, 8, and 12 hrs). Their absorbance was measured by using a Spectrometer.

3.9 Comparison of WHAC and Catalyst Performance at Same Parameters

The dye removal performance of WHAC and catalyst was measured at optimum value based on BBD optimization result, by using the same values of catalyst dose, dye concentration, and contact time independently based on BBD optimization result. To compare the dye removal performance of WHAC with the catalyst, the experiment was conducted with the same procedure except the adsorption experiment was conducted without UV light in the case of WHAC.

CHAPTER FOUR

4. RESULTS AND DISCUSSION

4.1 Proximate Analysis of WHAC

The proximate analysis result performed on WHAC is reported in Table 4-1.

Table 4-1 proximate analysis for WHAC.

No.	Characteristics	Values (%)
1	Moisture Content	3.1
2	Ash Content	12.5
3	Volatile Content	38
4	Fixed Carbon	46
5	Yield	41

4.1.1 Moisture Content

The moisture content of WHAC was 3.1%. This value is very diminutive. Smaller moisture content increases the adsorption capacity of carbon by giving strength to the action of AC. This value is within the moisture content values of the most prepared activated carbon samples and suitable for adsorption, since its surface is not occupied by water [92]. The moisture content decrease with increase pyrolysis temperature as more fluid particles and combustibles are driven off with greater heat intensity [93]. The moisture content of raw WHB (wet basis) has been 74.21% [Appendix I].

4.1.2 Ash Content

The ash content of the WHAC was 12.5%. This value is comparable to many similar studies and is within an acceptable range. Acid activation is responsible for the reasonable amount of ash content as it can reduce the ash content during the activation [94]. Low ash content is an indicator of high purity activated carbon [95]. Ash interfere with adsorption and catalysis of organic pollutants as it creates inactive sites [96]. The presence of excessive ash can lead to blocking of the pores on the activated carbon so that the surface area of activated carbon becomes reduced [97]. In general, low ash content indicates, the raw material used can be a good source for AC production [98].

4.1.3 Volatile Matter

The volatile matter of the activated carbon was 38%. The amount of volatile matter is relatively

higher probably because of the relatively low activation temperature. At lower activation temperature the detachment and decomposition of volatile matters from the base carbon will be lower thus there remains large quantities of volatile matter in the AC [99]. This is due to the higher pyrolysis temperatures of lignocellulosic material components, so that the decomposition of temperatures contained in raw materials such as water, tar, and volatile materials also higher [100]. Activators will free non-carbon elements, especially hydrogen, oxygen and nitrogen in liquid form known as tar and gases [101].

4.1.4 Fixed Carbon

As shown in Table 4.1 the amount of the fixed carbon is 46 %. The decrease in carbon content can be attributed to the higher volatile content of the AC. If the volatile matter is high, the proportion of free carbon in the AC becomes low, Reaction between the carbon and the activator at high concentrations can also reduce the amount of free carbon in the synthesized AC [102].

4.2 Characterization of photo catalyst

4.2.1 XRD -result

Figure 4-1 illustrates the XRD patterns of WHAC and TiO_2/WHAcc materials that were prepared by chemical activation and sol-gel method respectively. The peaks in the XRD analysis at 7.61°, 23.17°, 24.18°, 26.73°, 30.52°, 33.33°, 45.54°, and 77.74° are the diffraction values of (002), (100), (102), (004), (103), (110), (112), (006), (201) and (114) planes of graphite phase which is in agreement with ICDD cross-reference PDF # 'S (00-056-0160). The peaks in the XRD for catalyst analysis indicates by diffraction lines at 2 Theta equal to 25.34°, 37.98°, 48.06°, 54.34°, and 62.73° are the diffraction values of (101), (004), (200), (105), and (204) which represents JCPDS data of anatase TiO_2 (# 21-1272). The results of XRD indicate that the synthesized TiO_2 existed in an anatase state and there were no peaks that could be attributed to the brookite or rutile forms. The calcination process was done at low temperatures, which is not suitable for the formation of the other two phases. Bahram et al. synthesized TiO_2 in an anatase state on activated carbon and did not observe a brookite or rutile phase [103]. The high performance of photocatalysis observed in this study for TiO_2/WHAcc suggests that a certain amount of crystalline phase of TiO_2 nanoparticles was loaded on the surface of the WHAC. The crystallinity and crystallite size of WHAC and TiO_2/WHAcc were calculated and found to be 70.63 and 79.23, respectively. The average crystallite size of nanoparticles was also estimated to be 11.39 and 16.38 nm for TiO_2/WHAcc and WHAC, respectively. The decrement crystalline size value of TiO_2/AC may be related to the presence of decomposition products of AC into the crystalline structure of TiO_2 [104].

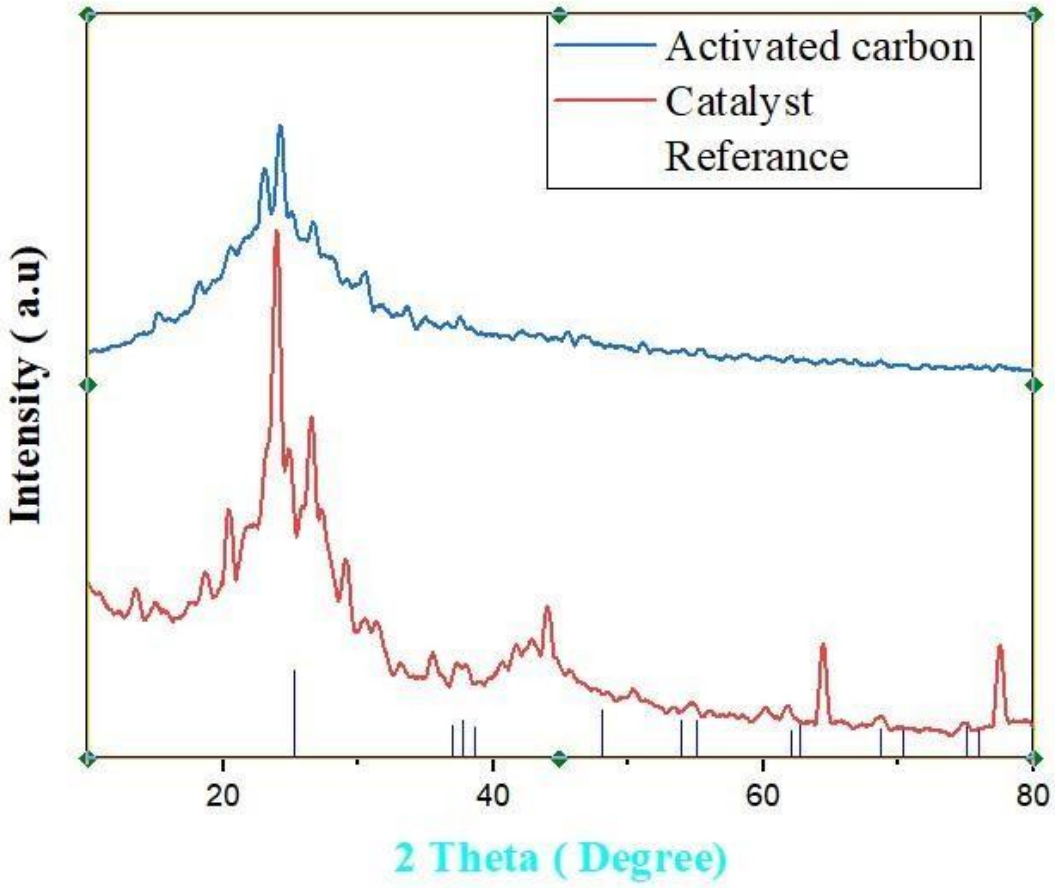

Figure 4-1 X-RD result of WHAC and catalyst

4.2.2 FT-IR result

The figure below shows the infrared absorption spectra (FT-IR) of WHAC and TiO_2 immobilized on WHAC catalyst. As can be observed from Figure 4-2, it has five main absorption bands in the wavelength of 4000-400cm^{-1}. The absorption peaks at 3700-3584cm^{-1} shows the stretching of intermolecular hydrogen bonds of O=H groups of WHAC and TiO_2/WHAC catalyst due to the adsorbed water. The other peak shows around 1746cm^{-1} correspond to the C=O bond which is normally found in the linkage of esters in the hemicellulose and lignin. The absorption bands of TiO_2/WHAcc at 1500-1000cm^{-1} were different from those of WHAC. This is caused by the Ti-O stretching vibrations. The absorption band at 1037cm^{-1} disappears because WHAC was covered by TiO_2 [105]. The FT-IR analysis gives evidence that TiO_2 has been loaded on WHAC.

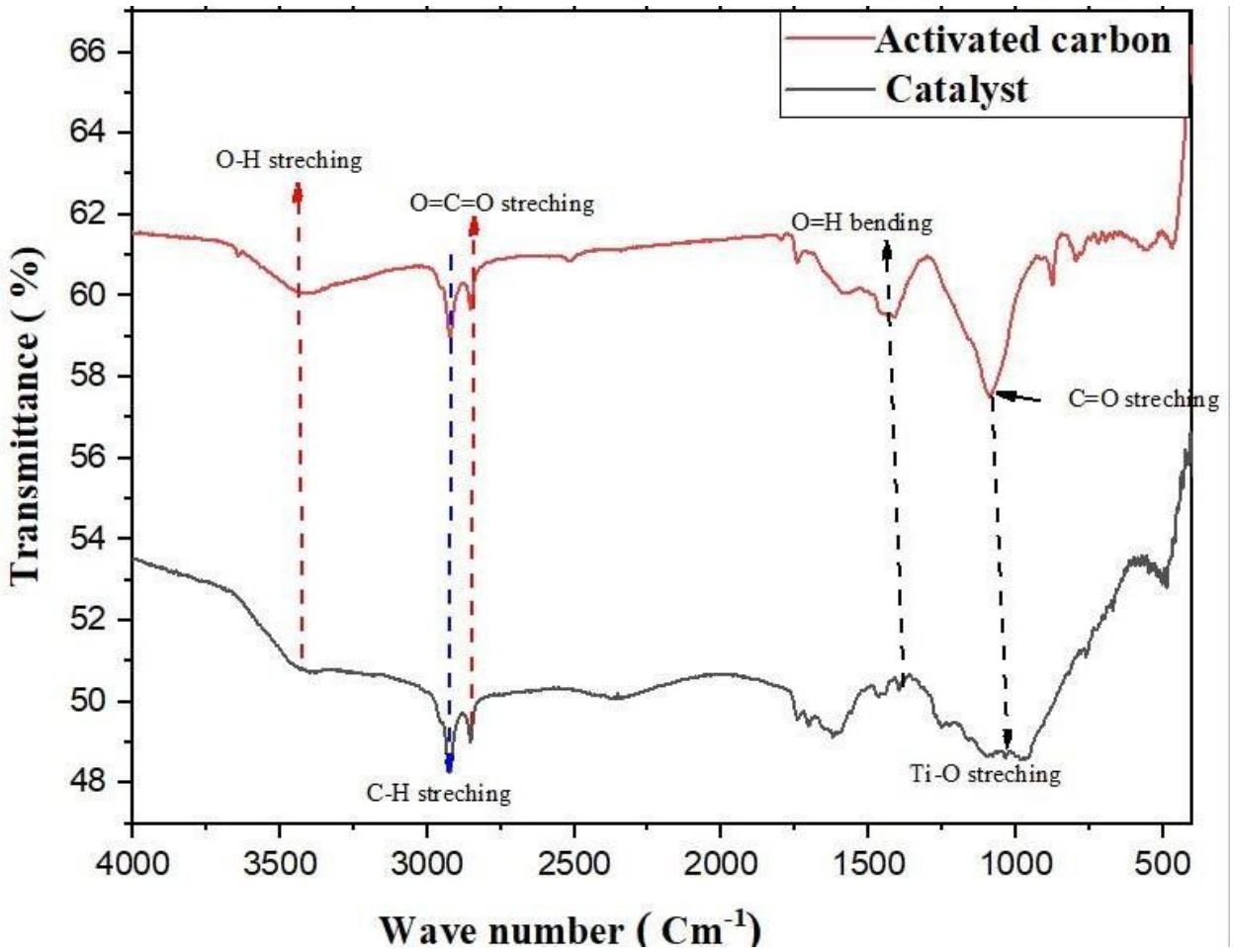

Figure 4-2 FT-IR spectra of WHAC and catalyst

4.2.3 Morphological result

Figure 4.3 shows SEM photomicrographs of the WHAC specimen before and after the immobilization of TiO_2 on the surface of WHAC. As can be seen form Figure 4.3A, WHAC (600°C) demonstrated a sheet like morphology which is in agreement with the graphitic phase, show by the XRD, of activated carbon. After impregnation and calcination as for the samples TiO2/WHAcc (4 and 12hrs.), the catalyst that was impregnated for (12 hrs.) has shown a rough surface which is composed of agglomerated TiO_2 nano-particles as has been confirmed by the energy dispersive X-ray (EDX) spectrum. However, in the case of the catalyst that was impregnated for (4hrs.), the sheet-like morphology is still apparent on SEM micrograph, Figure 4.3C, and the composition of Ti in the EDAX analysis was also significantly small. The result indicates the direct relationship between the impregnation time and the amount of TiO_2

incorporation with the AC.

Since TiO_2 is responsible for the photo catalytic effect of the catalyst, higher TiO_2 content on the AC surface will favor the catalytic performance enhancement. The analysis also confirmed a trace amount of phosphorus and a high amount of C and O_2. In the case of phosphorus, it was used as an activator for WHS but, due to continuous washing with distilled water, small amount of phosphorus was achieved. The C was due to simultaneous activation with phosphoric acid, more AC existed in the form of carbon.

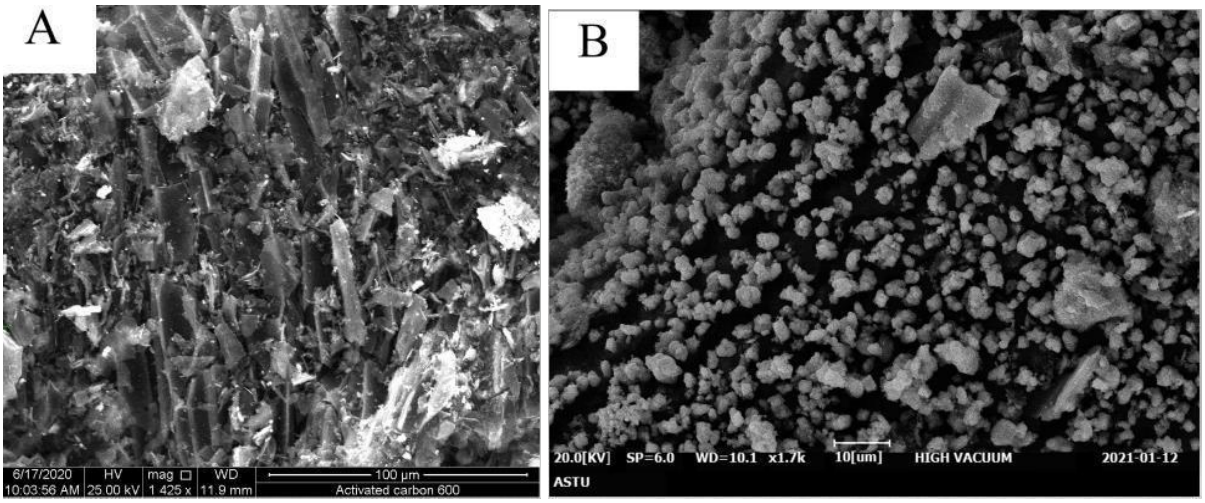

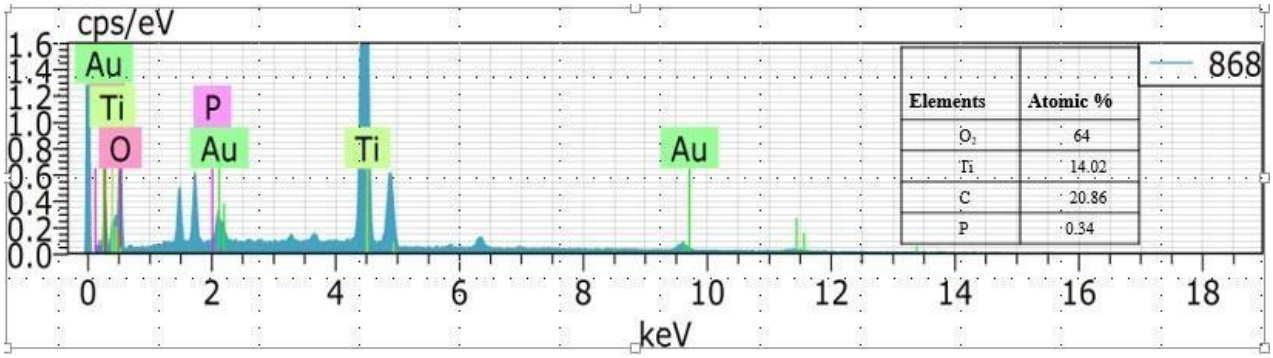

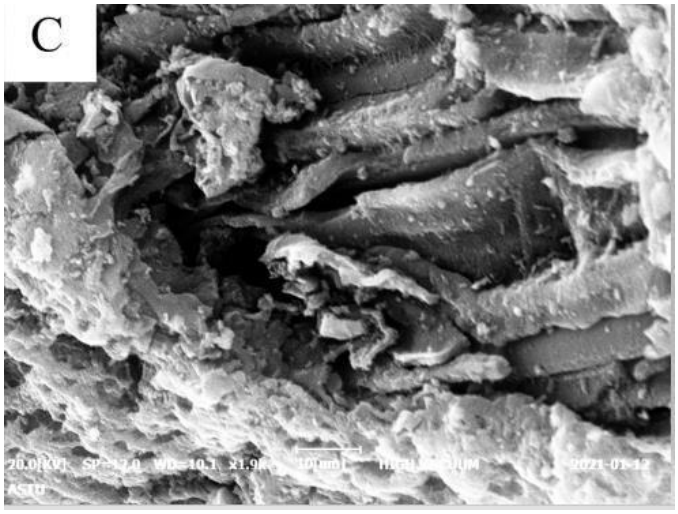

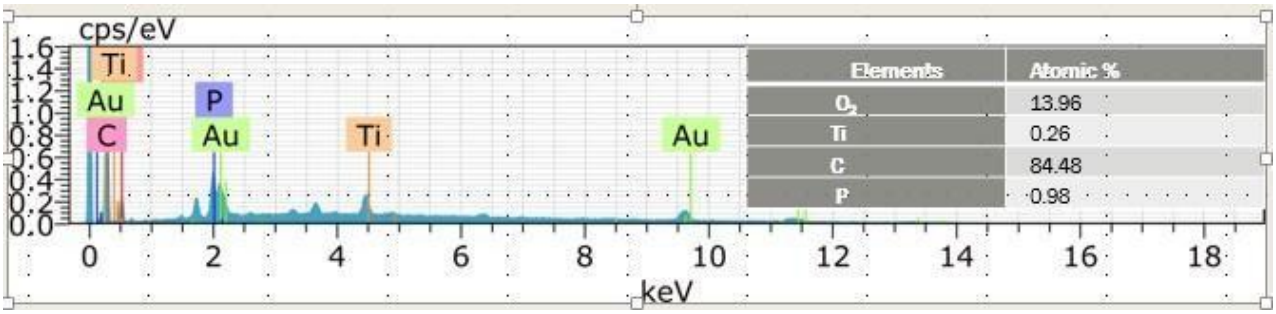

Figure 4-3 SEM images of (A) WHAC, (B and C), SEM images with EDX of TiO_2/WHAcc (12 and 4 hrs.) respectively.

4.2.4 Surface Area and pore development result

The BET surface areas of WHAC and TiO_2/WHAcc were 313.969 m^2/g and 279.757 m^2/g respectively. It is clear that coating WHAC with TiO_2 significantly reduces the BET surface area. This is mainly due to the blockage of the pore entries of WHAC by deposited TiO_2 particles and partly due to the agglomeration of TiO_2 into bigger particles. The total pore volume of the WHAC and TiO_2/WHAcc was 0.920 and 0.854cm^3/g respectively. This decrement indicates that some pores were blocked by TiO_2 particles. Since a large amount of internal surface of activated carbon is occupied by TiO_2 particles, TiO_2/WHAcc still shows high photocatalytic reactions. Wang, X., Liu reported the same result when studying the degradation of methyl orange by composite photocatalyst nano-TiO_2 immobilized on activated carbons of different porosities [106]. Another study shows that, the TiO_2 particles can block the activated carbon particles pore so its pore fraction decreased [107]. The detailed information was given in (Appendix J).

Table 4-2 Nitrogen Adsorption data for WHAC and TiO2/WHAcc

Parameters	**Value**	
	WHAC	TiO_2/WHAcc
Surface area (m^2/g)	313.969	279.757
Pore size (A^o)	36.435	34.076
Pore volume (cm^3/g)	0.920	0.854

4.3 Efficient WHAC selection

According to the selection experiment WHAC with (45% concentration and 600℃) was selected as the best adsorbent, for detailed information see (Appendix C).

Table 4-3 The removal efficiency of WHAC

Sample	**Final dye concentration** $c = \frac{A - 0.381}{0.0322}$	**Removal efficiency**
WHAC (400°C with 25% H_3PO_4)	4.25	71%
WHAC (400°C with 35% H_3PO_4)	2.07	75%
WHAC (400°C with 45% H_3PO_4)	2.1	86%
WHAC (600°C with 25% H_3PO_4)	3.9	73.4%
WHAC (600°C with 35% H_3PO_4)	3.5	76%
WHAC (600°C with 45% H_3PO_4)	0.52	96%
WHAC (800°C with 25% H_3PO_4)	0.590	70%
WHAC (800°C with 35% H_3PO_4)	3	75%
WHAC (800°C with 45% H_3PO_4)	2.08	94%

4.4 Efficient catalyst selection

According to the selection experiment, WHAC with (45% concentration and 600℃) was selected as the best adsorbent, for detailed information see (Appendix C).

Table 4-4 the removal efficiency of the catalyst

Adsorbents	Removal efficiency (%)
TiO_2/WHAcc (4 hr.)	77.8
TiO_2/ WHAcc (8 hr.)	89.8
TiO_2/WHAcc (12 hr.)	90.3

4.5 Statistical Analysis of the Experimental Results

4.5.1 Experimental Data

After the experimental work, the removal efficiency was calculated at the different ranges and analyzed with the software. The results from RSM were discussed in the following section.

Table 4-5 BBD matrixes of independent variables used in RSM with corresponding

Run No	Factor 1	Factor 2	Factor 3	Removal efficiency (%)	Removal efficiency (%)
	A: dose (gm)	B: contact time (min)	C: dye concentration (gm^{-L}	Actual	Predicted
1	0.1	15	10	99.47	99.33
2	0.1	45	20	85.37	85.51
3	0.05	30	10	78.30	78.10
4	0.1	30	15	90.80	90.80
5	0.05	45	15	70.60	70.79
6	0.15	15	15	99.90	99.71
7	0.15	30	20	93.00	93.20
8	0.1	30	15	90.80	90.80
9	0.05	30	20	70.70	70.37
10	0.15	45	15	70.10	69.76
11	0.05	15	15	71.50	71.84
12	0.15	30	10	81.80	82.12
13	0.1	30	15	90.80	90.80
14	0.1	15	20	92.00	91.99
15	0.1	45	10	74.80	75.81

4.5.3 Model Summary Statics

In this study RSM based on BBD was used to investigate the effect of catalyst dosage, contact time, and dye concentration on the removal of MB using design-expert software 7.0. The statistical significance of the model was analyzed using ANOVA as shown in Table 4-7.

Table 4-6 Analysis of variance (ANOVA) result for the photocatalytic experiment

Source	Sum of Squares	df	Mean Square	F-value	p-value	
Model	1604.98	9	178.33	1420.97	< 0.0001	significant
A-dose	360.46	1	360.46	2872.20	< 0.0001	
B-Contact Time	480.50	1	480.50	3828.69	< 0.0001	
C-Dye concentration	5.61	1	5.61	44.71	0.0011	
AB	208.80	1	208.80	1663.76	< 0.0001	
AC	88.36	1	88.36	704.06	< 0.0001	
BC	81.36	1	81.36	648.29	<0.0001	
A^2	359.51	1	359.51	2864.63	< 0.0001	
B^2	31.21	1	31.21	248.71	< 0.0001	
C^2	0.0011	1	0.0011	0.0090	0.9281	
Residual	8.44	5	1.69			
Lack of Fit	8.44	3	2.81			
Pure Error	0.0000	2	0.0000			
Cor Total	1501.39	14				

The **Model F-value** of 1420.97 implies the model is significant. There is only a 0.01% chance that an F-value this large could occur due to noise. **P-values** less than 0.0500 indicate model terms are significant. In this case, A, B, AB, AC, BC, A^2, B^2 are significant model terms. Values greater than 0.1000 indicate the model terms are not significant. If there are many insignificant model terms (not counting those required to support hierarchy), model reduction may improve your model [108]. From ANOVA we can conclude that the initial dye concentrations range which was (10, 15, and 20mgL^{-1}), maybe was not enough to see the effect of this parameter on the removal efficiency, but if we increase the dye concentration range, it will be enough to see this parameter on dye removal efficiency.

Table 4-7 A suggested model for the design

Statistical Property	**Value**
Std.Dev	0.3543
Mean	84.00
C.V.%	0.4218
R^2	0.9996
Adjusted R^2	0.9998
Predicted R^2	0.9937
Adeq. Precision	103.5430

The **Predicted R²** of 0.9937 is in reasonable agreement with the **Adjusted R²** of 0.9989; that is, the difference is less than 0.2. **Adeq Precision** measures the signal-to-noise ratio. A ratio greater than 4 is desirable. Your ratio of 103.543 indicates an adequate signal. This model can be used to navigate the design space.

4.5.4 Diagnostic Plot

Furthermore, the adequacy model can be investigated by plotting some diagnostic adequacy plots such as normal % plot, standardized plot, and predicted versus actual plots were shown in Fig 4-4.

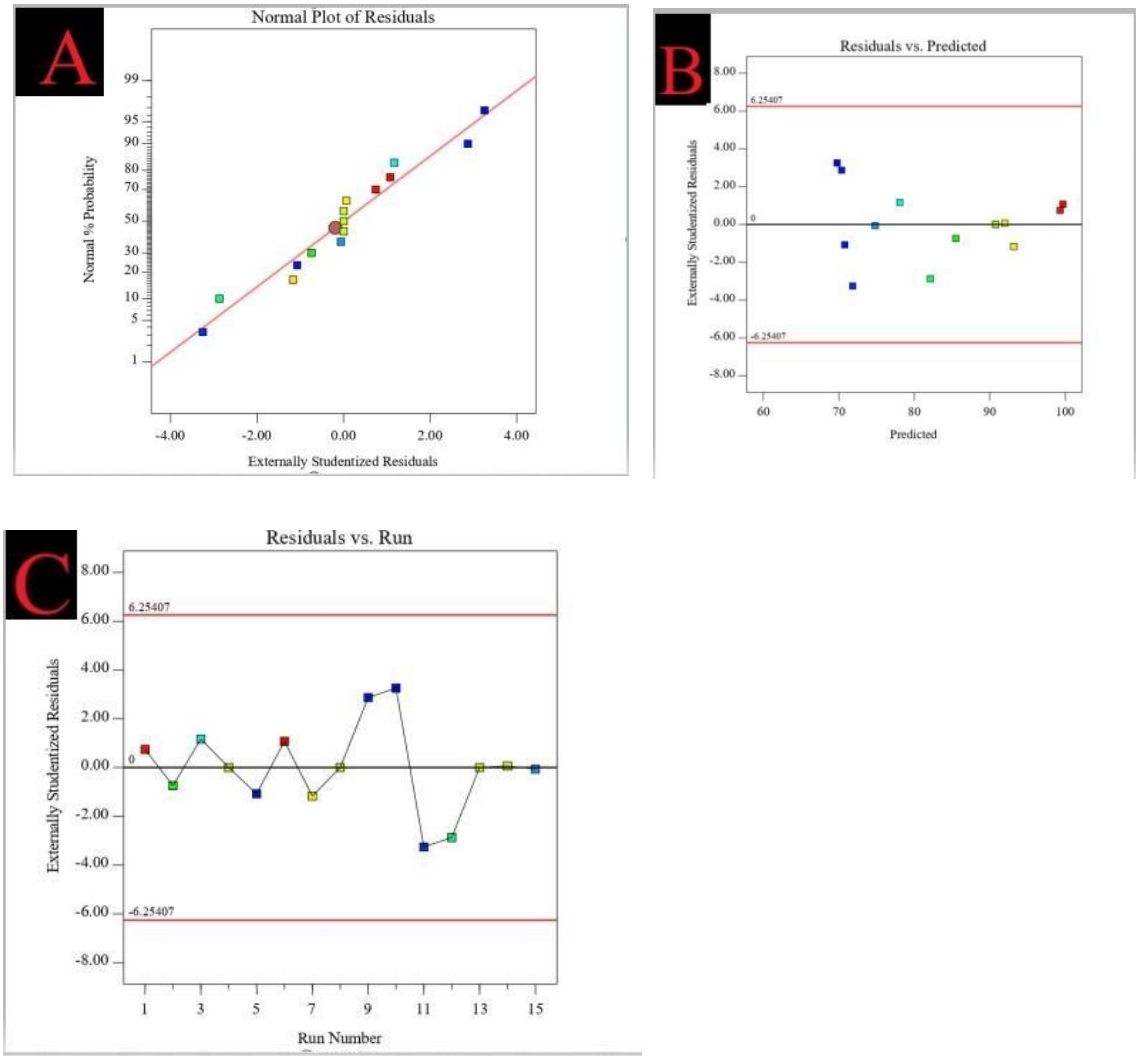

Figure 4-4 Diagnostic plots for the photocatalytic experiment

Based on the regression analysis the quadratic model equations for one response dye removal efficiency for a photocatalytic experiment in terms of actual values can be written by considering only the significant model terms (see equation 4.1).

Removal efficiency =+ [67.43000 + 853.65000 A+ 0.063333B − 2.87750C − 8.16667A∗

B+ 18.80000A ∗ C+ 0.060133B∗ C− 3.727.00000A^2 − 0.010478B^2 − 0.021300C^2

The equation in terms of actual factors can be used to make predictions about the response for given levels of each factor. Here, the levels should be specified in the original units for each factor. This equation should not be used to determine the relative impact of each factor because the coefficients are scaled to accommodate the units of each factor and the intercept is not at the center of the design space.

4.5.5 The interaction effect of process variables on the photocatalytic performance

1) Interaction of catalyst dose and dye concentration on removal efficiency

Figure 4-5: illustrates the interaction of catalyst dose and dye concentration on the decolorization rate. By increasing the amount of catalyst, the number of the available active site on the catalyst surface increase, which in turn leads to an increase in the number of hydroxyl and superoxide radicals [109]. The probability of formation of OH^- radicals reacting with dye molecules determine the degradation rate [110]. As the initial dye concentration increase, more dye molecules are available for excitation and energy transfer. This dependence is perhaps related to the formation of several monolayers of adsorbed dye on the TiO_2 surface, which is favored at high dye concentrations. The catalyst dose and dye concentration has positive interaction, which fits with literatures [111]. A balance between the dye molecules and the hydroxyl radical is the key requirement for the effective degradation [112].

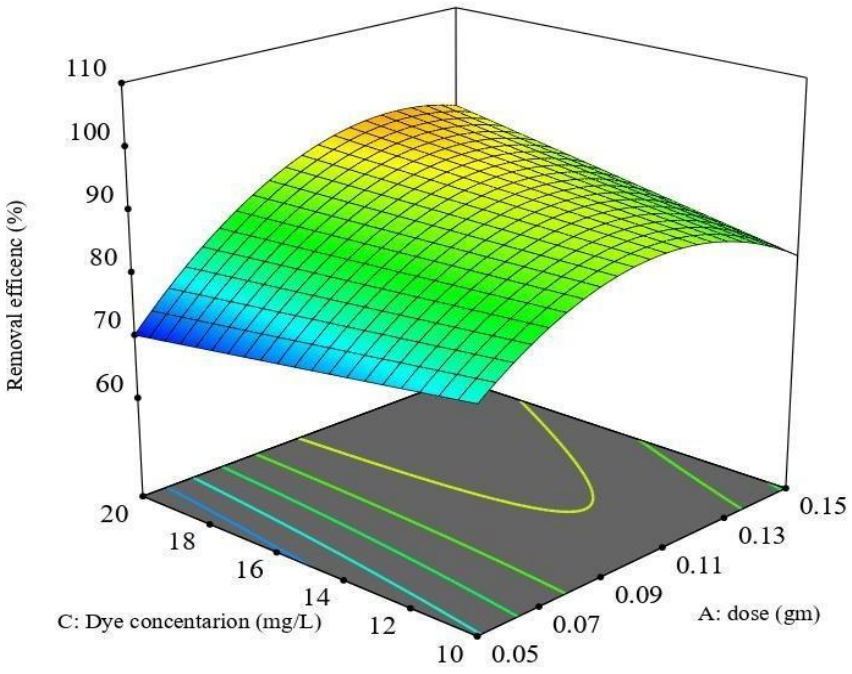

Figure 4-5 Interaction of catalyst dose and dye concentration on removal efficiency

2. Interaction of contact time and catalyst dose

Contact time and catalyst dose had an interaction effect as shown in Figure 4.6, according to the 3D graph, the combined effect of adsorbent dose and contact time at constant dye concentration. The adsorbent dose with contact time an increase of response function (% removal) of methylene blue was observed. This is because of the adsorbent active sites availability increase with elevation of contact time and thus higher adsorption of methylene blue dye from the solution onto adsorbent [113]. The reason can be relevant to the enhancement of active sites on the surface of catalysts to capture more hydroxyl and superoxide radicals and, finally, absorbance of more methylene blue molecules. The enhancement of the effect of the applied dose in the removal of dye with increasing the time intervals related to the associated increase in the amount of adsorbed methylene blue dye with increasing contact time, so contact time and catalyst does have positive interaction [114].

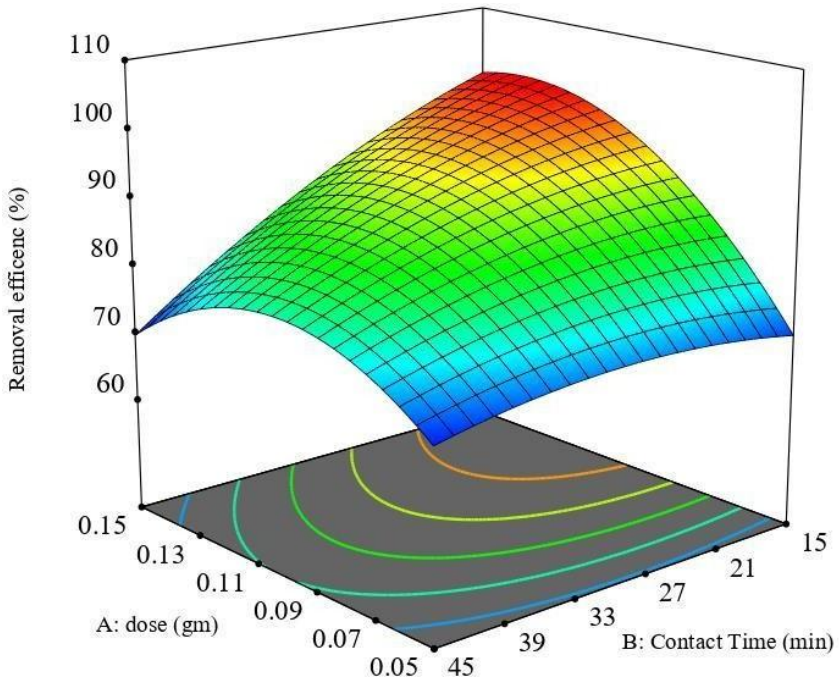

Figure 4-6 Interaction of contact time and catalyst dose

3. Interaction effect of contact time and dye concentration

As shown in Fig. 4.7, if we minimize the dye concentration there may have little interaction effect but, in the figure below, contact time and dye concentration didn't have interaction. As a result, the variation of contact time didn't affect dye concentration.

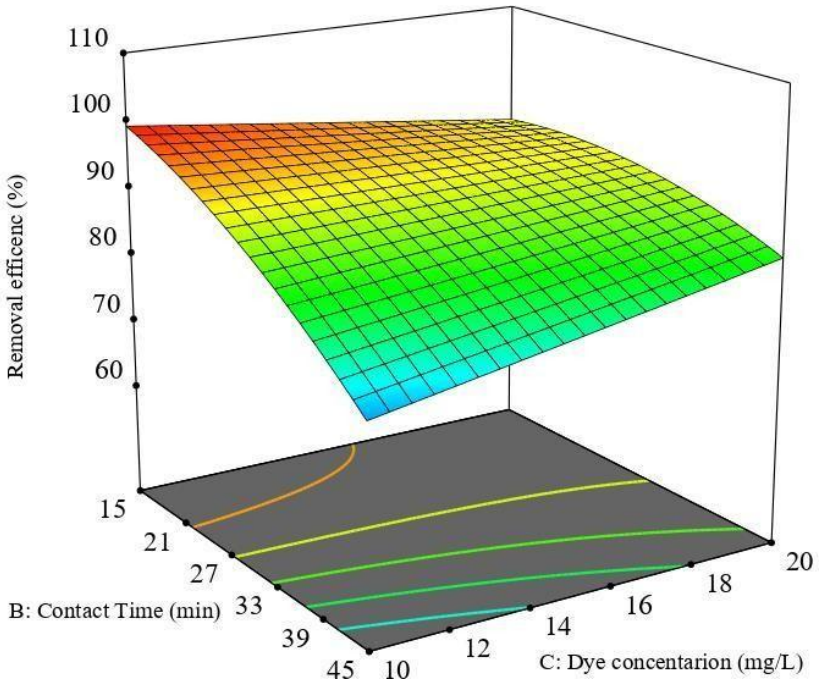

Figure 4-7 Interaction effect of contact time and catalyst dose

4.6 Optimization of the Process Parameters and Verification

The efficient catalyst was selected using numerical optimization for maximum removal efficiency at minimum dosage, maximum dye concentration for a given range of contact time according to Table 4-9.

Table 4-8 Constraints to select the best catalyst

Name	Goal	Lower Limit	Upper Limit	Lower Weight	Upper Weight	Importance
A: dose	minimize	0.05	0.15	1	1	3
B: Contact Time	in range	15	45	1	1	3
C: Dye concentration	maximize	10	20	1	1	3
Removal efficiency	maximize	70.6	99.9	1	1	3

From, the numerical optimization results in Table 4-9, dye concentration of 20 mgL^{-1}, catalyst dose 0.092gm, and contact time 24.598 min were selected with 0.669 desirability to predict the maximum dye removal efficiency of 91.05%. The result was also validated with three test runs and the result was obtained 91.05 ±0.42, which is very close to the predicted optimum value of the removal efficiency. The optimum removal efficiency of the prepared catalyst material also compares with the raw activated carbon and its efficiency was found lower by about 20% (Table 4.9). From the result, we can conclude that the addition of TiO_2 nanoparticles can significantly improve the removal efficiency of the activated carbon.

Table 4-9 Comparison of WHAC and TiO_2/WHAcc

Adsorbent dosage (gm)	Dye concentration (mg/L)	Contact time (min.)	Dye removal WHAC	Efficiency Catalyst
0.092	20	24.589	72.25 %	91.05 %

CHAPTER FIVE
5. CONCLUSION AND RECOMMENDATION

5.1 Conclusion

In the present work, the synthesis and characterization of activated carbon from WH (Emboch) by chemical activation using different temperatures (400,600,800°C) and activating agent phosphoric acid (H_3PO_4) with different concentrations (25,35 and, 45 %) were investigated. The catalyst using the sol-gel method, titanium butoxide as a precursor of TiO_2, and its application for the removal of MB were investigated. The experimental results showed that TiO_2/WHAcc was influenced by impregnation time. The photocatalytic optimization was done using the Box-Behnken response surface methodology and by taking MB concentration, catalyst dose, and contact time as constraints, 91.05% MB removal efficiency was obtained. The XRD result revealed that TiO_2 has only an anatase phase and carbon was in the form of graphite. Immobilization of TiO_2 on the surface of WHAC significantly reduces the BET surface area and total pore volume due to blockage of the pore entries of WHAC by the deposited TiO_2 particles and due to agglomeration of TiO_2 into bigger particles. From FT-IR analysis the desired functional groups were determined for WHAC and catalyst which justified that the impregnation of TiO_2 onto the surface of WHAC. The absorption peak at 1037 cm^{-1} disappears due to the Ti-O stretching vibration. Surface morphology WHAC and TiO_2/WHAcc were analyzed by FE-SEM and elemental composition using EDX. The WHAC (600°C for 45%) impregnation time revealed that a smooth surface was observed due to simultaneous activation with H_3PO_4. The case of the catalyst that was impregnated for (12 hrs.) revealed that TiO_2 was well dispersed on the surface of AC and the high content of TiO_2 was achieved. While the other catalyst that was impregnated for (4 hrs.) revealed that TiO_2 was formed agglomerate and a relatively small amount of TiO_2 was achieved. In summary, the TiO_2/WHAcc sample has higher removal efficiency compared to WHAC.

5.2 Recommendations

TiO_2/WHAcc was an efficient catalyst for MB dye removal. The following recommendation had improved the synthesis of a catalyst by the researchers

- In this thesis work, activated carbon was prepared from the water hyacinth stem, but the future studied needed to produce activated carbon from water hyacinth leave and root.
- The water hyacinth-based activated carbon was prepared at different temperatures (400,600,800°C) but for only 2 hrs. carbonization time to make the study more compressive, it is better to activate carbon at different carbonization times.
- The catalyst was prepared at different impregnation times but it's better to study at different impregnation ratios with different calcination temperature.

REFERENCE

1. Ramakrishna "Biomimetic Synthesis of Hybrid Materials for Potential Applications Mallampati (M. Sc. University of Pune, India) For the Degree of Doctor of Philosophy Department of Chemistry," 2013.
2. Philippe Gourbesville, "Challenges for integrated water resources management," Physics and Chemistry of the Earth 33 (2008) 284–289, 2008, doi: 10.1016/j.pce.2008.02.002.
3. Iftikhar Ahmad, Muhammad Imran, "Remediation of organic and inorganic pollutants from soil: The role of Plant-Bacteria Partnership," 2017, p. 197-243.
4. Ms. R. Priya Dharshini and Dr. V. Judia Harriet Sumathy, "Biodegradation of Textile Azo Dyes using Fungi," International Journal of Medicine and Pharmaceutical Research, Vol.2 (3): 611-621, 2014.
5. Mohamed A. Hassaan, Ahmed El Nemr. "Health and Environmental Impacts of Dyes: Mini Review," American Journal of Environmental science and Engineering, Vol. 1, No. 3, 2017, pp. 64-67. doi: 10.11648/j.ajese.20170103.11
6. Renmin Gong, Yingzhi Suna , Jian Chenb , Huijun Liua , Chao Yang "Effect of chemical modification on dye adsorption capacity of peanut hull", Elsevier, Volume 67, 2005, Pages 175-18, https://doi.org/10.1016/j.dyepig.2004.12.003.
7. Bruno Lellis, Cintia Zani Favaro-Polonio, Joao Alencar Pamphile, "Effects of textile dyes on health and the environment and bioremediation potential of living organisms," Biotechnology Research and Innovation, October 2019, https://doi.org/10.1016/j.biori.2019.09.001.
8. Bewuket Teshome Wagaye, and Gashaw Ashagre Walle, "Overview of Ethiopian Textile Industry," JOURNAL OF TEXTILES AND POLYMERS, Ethiopian Institute of Textile and Fashion Technology, Bahir Dar, Ethiopia. VOL. 6, NO. 2, JUNE 2018.
9. P. Tarapitakcheevin, P. Weerayutsil, and K. Khuanmar, "Adsorption of Acid Dye on Activated Carbon Prepared from Water Hyacinth by Sodium Chloride Activation," Greater Mekong Subregion Academic and Research Network, 2013.
10. Arielle Tonus Ellis, "Water Hyacinth, *Eichhoria crassipes*", 2011.
11. Vanessa D. Tobias, J. Louise Conrad, Brian Mahardja, Shruti Khanna, "Impacts of water hyacinth treatment on water quality in a tidal estuarine environment," Biol Invasions (2019) 21:3479–3490, https://doi.org/10.1007/s10530-019-02061-2.

12. Minychl G. Dersseh, Assefa M. Melesse, Seifu A. Tilahun, Mengiste Abate, and Dessalegn C. Dagnew "Water hyacinth: review of its impacts on hydrology and ecosystem services-Lessons for management of Lake Tana," 2019, https://doi.org/10.1016/B978-0-12-815998-9.00019-1.
13. Prof. Rahul Udata, Prajakta Shinde, Shubham Shewale, Shradha Yelavi, and Vikas Tripathi, "QUANTIFICATION OF WATER HYACINTH IN P.C.M.C. AREA BY GIS AND ASSESSMENT OF METHODS OF MANAGEMENT," INTERNATIONAL JOURNAL OF ADVANCE SCIENTIFIC RESEARCH & ENGINEERING TRENDS, Volume 5, IMPACT FACTOR 6.228, May 2021.
14. Abera Hailu Degaga, "Water Hyacinth (Eichhornia crassipes) Biology and Its Impacts on Ecosystem, Biodiversity, Economy and Human Well-being," Journal of Natural Sciences Research, Vol.9, No.12, 2019, DOI: 10.7176/JNSR.
15. A. M. Villamagna and B. R. Murphy, "Ecological and socio-economic impacts of invasive water hyacinth (Eichhornia crassipes): a review," Freshwater Biology, pp: 282–298, 2010, doi:10.1111/j.1365-2427.2009.02294. x.
16. Kathryn Terblanch, Errol Douwes, "Water Hyacinth Control: Insight into Best Practice, Removal Methods, Training & Equipment," 2013, DOI: 10.13140/RG.2.1.1367.5041.
17. SAGAR MUKUNDRAO GAWANDE, NIHARIKA SURESH BELWALKAR, ANUJA ASHOK MANE, "Production of Produced Activated Pac from Water Hyacinth (Eichhronia Crassipes) Whpac," 2015.
18. Krzysztof Piaskowski, Renata Swiderska-Dabrowska, and Pawel K. Zarzycki, "Dye Removal from Water and Wastewater Using Various Physical, Chemical, and Biological Processes," Journal of AOAC International vol. 101, No. 5, 2018, DOI: https://doi.org/10.5740/jaoacint.18-0051.
19. C. Andriantsiferanaa, E.F. Mohamedb, "Photocatalytic degradation of an azo-dye on TiO2/activated carbon composite material," Environmental Technology,2014, Vol. 35, No. 3, 355–363, http://dx.doi.org/10.1080/09593330.2013.828094.
20. Gregorio Crini, Eric Lichtfouse, Lee Wilson, Nadia, and Morin-Crini, "Green Adsorbents for Pollutant Removal," Removal, Environmental Chemistry for a Sustainable World 18. Springer, pp. 23-71,2018, https://doi.org/10.1007/978-3-319-92111-2.

21. Kaleem Ahmad, Himadri Roy Ghatak, " Photocatalytic Technology: A review of environmental protection and renewable energy application for sustainable development," Environmental Technology and Innovation, 2020, DOI: https://doi.org/10.1016/j.eti.2020.100893.
22. S. Cassaignon, C. Colbeau-Justin and O. Durupthy, "Titanium Dioxide in Photocatalysis," Nanomaterials, Springer-Verlag London, 2013, DOI: 10.1007/978-1-4471-4213-3_6.
23. D Reyes-Coronado, G Rodrıguez-Gattorno, M E Espinosa-Pesqueira, C Cab1, R de Coss1 and G Oskam, "Phase-pure TiO_2 nanoparticles: anatase, brookite, and rutile," *International on Inventive Research in Material Science and Technology*, 2008, doi:10.1088/0957-4484/19/14/145605.
24. Haoran Dong, Guangming Zeng, Lin Tang, Changzheng Fan, Chang Zhang, Xiaoxiao, and Yan He, "An overview on limitations of TiO_2-based particles for photocatalytic degradation of organic pollutants and the corresponding counter measures," www.elsevier.com/locate/watres,128 146,2015.
25. N. J. Peill and M. R. Hoffmann, "Chemical and physical characterization of a TiO_2-coated fiber optic cable reactor," Environmental Science and Technology, vol. 30, no. 9, pp. 2806–2812, 1996.
26. Bahram Ghasemi, Bagher Anvaripour, Sahand Jorfi, and Neematollah Jaafarzadeh, "Enhanced Photocatalytic Degradation and Mineralization of Furfural Using UVC/TiO_2/GAC Composite in Aqueous solution," International Journal of Photoenergy, Article ID 2782607, 2016, http://dx.doi.org/10.1155/2016/2782607.
27. Khan, I.; Saeed, K.; Zekker, I.; Zhang, B.; Hendi, A.H.; Ahmad, A.; Ahmad, S.; Zada, N.; Ahmad, H.; Shah, L.A.., "Review on Methylene Blue: Its Properties, Uses, Toxicity and Photodegradation," Water 2022, 14, 242. https://doi.org/ 10.3390/w14020242
28. Tiantian Liu, Zhen Wang, Xinrui Wang, Guihua Yang , Yu Liu, " Adsorption-photocatalysis performance of polyaniline/dicarboxyl acid cellulose@graphene oxide for dye removal," International Journal of Biological Macromolecules, https://doi.org/10.1016/j.ijbiomac.2021.04.038, 2021.

29. Shailendra Mohan Mathur, “Water hyacinth (*(Eichhornia crassipes)* Choppercum Crusher: A Solution for Lake Water Environment", Journal of Energy Technologies and Policy, vol.3, No.11, 2013.
30. Tariq Mahmood, Syed Tajammul Hussain, and Salman Akbar Malik, “New nanomaterial and process for the production of biofuel from metal hyper accumulator water hyacinth,” African Journal of Biotechnology Vol. 9(16), pp. 2381-2391, 19 April, 2010.
31. Suchi Tiwari & Savita Dixit & Neelam Verma, “An Effective Means of Biofiltration of Heavy Metal Contaminated Water Bodies Using Aquatic Weed Eichhornia crassipes,” Environ Monit Assess (2007) 129:253–256, DOI 10.1007/s10661-006-9358-7.
32. Matai S, Bagchi DK, “Water hyacinth: a plant with prolific bio-productivity and photosynthesis,” process International Symposeyum on Biological application of Solar energy: p. 113, 1980.
33. Gohl B, “Tropical feeds. Feed information summaries and nutritive values. FAO Animal Production and Health Series,” 12 FAO, Rome, 1981.
34. Sivasankari. B, David Ravindran.A, “A Study on Chemical Analysis of Water Hyacinth (*Eichhornia crassipes*), Water Lettuce (*Pistia stratiotes*),” International Journal of Innovative Research in Science, Engineering and Technology, vol.5, Issue 10, 2016, DOI:10.15680/IJIRSET.2016.0510010.
35. Abn Fadoua Karouach, Amine Ezzariai,,“ A Comprehensive Evaluation of the Existing Approaches for Controlling and Managing the Proliferation of Water Hyacinth (Eichhornia crassipes): Review” Article in Frontiers in Environmental Science,2022, DOI: 10.3389/fenvs.2021.767871.
36. Aman Kumar Gupta, Dipak Yadav, “BIOLOGICAL CONTROL OF WATER HYACINTH,” Environmental Contaminants Reviews (ECR), 2020, DOI: http://doi.org/10.26480/ecr.01.2020.37.39.
37. Alireza Mirzajani, Noshin Nezamabadi, “Chemical control of water hyacinth by some herbicides and their effect on some aquatic invertebrate”,2022, DOI: https://doi.org/10.21203/rs.3.rs-1242651/v1.
38. O. E. Omofunmi, S. A. Ebifemi, and A. B. Eweina, “ Design of Water Hyacinth (Eichhornia crassipes) Harvester,” Journal of Scientific Research & Reports 10(5): 1-10, 2016; Article no.JSRR.24858 ISSN: 2320-0227, DOI: 10.9734/JSRR/2016/24858.

39. Harley, L. S., Julien, M. H., and Wright, A. D., "Water Hyacinth: A Tropical Worldwide Problem and Methods for its Control, Proceedings of the first meeting of the International Water Hyacinth Consortium," March 1997.
40. Dr.engHebatalrahman, "Titanium Data base part 1," https://www.researchgate.net/publication/316636275, 2017.
41. Hadi Nugraha Cipta Dharma, Juhana Jaafar, "A Review of Titanium Dioxide (TiO_2)-Based Photocatalyst for Oilfield-Produced Water Treatment," 2022, https://doi.org/10.3390/membranes12030345.
42. Sofian Kanan, Matthew A, "Recent advances on TiO_2-based photocatalysts toward the degradation of pesticides and major organic pollutants from water bodies," Catalyst Reviews Science and Engineering, 2019, DOI: 10.1080/01614940.2019.1613323.
43. Agatino Di Paola, Marianna Bellardita, "Brookite, the Least Known TiO_2 Photocatalyst," Catalysts 2013, 3, 36-73; doi: 10.3390/catal3010036.
44. Elisa I. Garcı´a-Lo´ pez, Leonardo Palmisano, "Fundamentals of photocatalysis: The role of the photocatalysts in heterogeneous photo-assisted reaction"2012, Materials Science in Photocatalysis. https://doi.org/10.1016/B978-0-12-821859-4.00004-0.
45. Kazuya Nakataa,b, Akira Fujishimaa, "TiO_2 photocatalysis: Design and applications," Journal of Photochemistry and Photobiology C: Photochemistry Reviews 13 (2012) 169–189, http://dx.doi.org/10.1016/j.jphotochemrev.2012.06.001, 2012.
46. Juanrong Chen, Fengxian Qiu Wanzhen, Xu Shunsheng Cao, Huijun Zhu,"Recent Progress in Enhancing Photocatalytic Efficiency of TiO2-based Materials," Applied Catalysis A: General, 2015, http://dx.doi.org/doi:10.1016/j.apcata.2015.02.013.
47. Dorian A. H. Hanaor, Charles C. Sorrell, "Review of the anatase to rutile phase transformation," J Mater Sci (2011) 46:855–874, DOI 10.1007/s10853-010-5113-0.
48. Tigabu Halefom, "Removal of Methylene Blue Dye Using Titanium Dioxide Photocatalyst", School of Chemical Engineering, Msc.Thesis, 2019, University of Addis Ababa Institute of Technology.
49. Chi Him A. Tsang, Kai Li, Yuxuan Zeng, Wei Zhao, Tao Zhang, Yujie Zhana, Ruijie Xie, Dennis Y.C. Leung, Haibao Huang, "Titanium oxide based photocatalytic materials development and their role of in the air pollutants degradation: Overview and forecast", environment International, https://doi.org/10.1016/j.envint.2019.01.015.

50. Hongbo Shi, Ruth Magaye, Vincent Castranova, Jinshun Zhao, "Titanium dioxide nanoparticles: a review of current toxicological data," Particle and Fibre Toxicology 2013, 10:15 doi: 10.1186/1743-8977-10-15.
51. Haoran Dong, Guangming Zeng, Lin Tang, Changzheng Fan, Chang Zhang, Xiaoxiao He, Yan He, "An overview on limitations of TiO_2-based particles for photocatalytic degradation of organic pollutants and the corresponding countermeasures",2015, http://dx.doi.org/10.1016/j.watres.2015.04.038.
52. M.A. Tadda1, A. Ahsan, "A review on activated carbon: process, application and prospects", Journal of Advanced Civil Engineering Practice and Research, https://www.researchgate.net/publication/318827940, 2017.
53. T.Subramani, P.K Revathi, "Production of Activated Carbon From Agricultural Raw Waste", IOSR Journals of Engineering (IOSRJEN), Vol.05, Issue 05(May),2015.
54. Zoha Heidarinejad1, Mohammad Hadi Dehghani, "Methods for preparation and activation of activated carbon: a review", Environmental Chemistry Letters (2020) 18:393–415, https://doi.org/10.1007/s10311-019-00955-0.
55. F.Rodriguez-Reinoso and M.MOLINA-SABIO, "Activated Carbons from Lignocellulosic Materials by Chemical and/or Physical Activation: Overview", Vol.30, No 7, 1992.
56. Nubia Rangel Candidoa, Marcos J. Prauchnerb, Adriana de Oliveira Vilelac, Vanya M.D. Pasa, "The use of gases generated from eucalyptus carbonization as activating agent to produce activated carbon: an integrated process", Journal of Environmental Chemical Engineering, 2020, https://doi.org/10.1016/j.jece.2020.103925.
57. Ping Feng, Li, Huan Wang, and Zhiqiang Xu, "Biomass-Based Activated Carbon and Activators: Preparation of Activated Carbon from Corncob by Chemical Activation with Biomass Pyrolysis Liquids", ACS Omega 2020, doi: https://dx.doi.org/10.1021/acsomega.0c03494.
58. Nibiret, Getasew, "Synthesis and Characterization of Activated Carbon from Water Hyacinth of Lake Tana for the Removal of Methylene Blue Dye from Textile WasteWater", Faculty of Chemical and Food Engineering, MSc. Thesis, 2017, University of Bahirdar Institute of Technology, http://hdl.handle.net/123456789/10625.
59. Zoha Heidarinejad, Mohammad Hadi Dehghani, Mohsen Heidari, Gholamali Javedan, Imran Ali, Mika Sillanpää, "Methods for preparation and activation of activated carbon:

a review," Environmental Chemistry Letters (2020) 18:393–415, https://doi.org/10.1007/s10311-019-00955-0.

60. Wanwu Li1, Farrukh Raza Amin, "Effects of Temperature, heating rate, residence time, reaction atmosphere, and pressure on Biochar properties," J. Biobased Mater and Bioenergy, Vol. 13, 1–10, 2019.
61. Puthiya Veetil Nidheesh, Rajan Gandhimathi, and Srikrishnaperumal Thanga Ramesh, "Degradation of dyes from aqueous solution by Fenton processes: a review," Environ Sci Pollut Res (2013) 20:2099–2132, DOI 10.1007/s11356-012-1385-z.
62. Iqbal M, "Textile dyes," Senior Research Associate, Textile PCSIR Laboratories complex Karachi Ministry of Science & Technology Government of Pakistan, MSc thesis, 2008.
63. Said Benkhaya, Sara El Harfi, and Ahmed El Harfi, "Classifications, properties and applications of textile dyes: A review," Appl. J. Envir. Eng. Sci, 2017.
64. M.S. Lucas, A.A. Dias, A. Sampaio, C. Amaral, J.A. Peres, Water Research 41 (2007) 1103–1109.
65. Anjaneyulu, Y.; Sreedhara, "Decolourization of industrial effluents – available methods and emerging technologies – a review," V ol.4, pp. 245-273, 2005, DOI 10.1007/s11157-005-1246-z.
66. V A. Simi and V. Azeeza, "Removal of methylene blue dye using low-cost adsorbent," Research Journal of Chemical Science, Vol. 4(1), 91-102, January (2014).
67. A. Da˛browski, "Adsorption from theory to practice," Adv. Colloid Interface Sci., (2001).
68. A.R.Warade, R.W.Gaikwad, R.S.Sapkal, and V.S.Sapkal, "STUDY OF REMOVAL TECHNIQUES FOR DYES BY ADSORPTION: A REVIEW," IJARIIE-ISSN (O)-2395-4396, Vol-2 Issue-3 2016.
69. Deepika Bhatia, Neeta Raj Sharma, "Biological methods for textile dye removal from wastewater: A review," Critical Reviews in Environmental Science and Technology, 2017, DOI: 10.1080/10643389.2017.1393263.
70. Bestani Benaouda, "The use of TiO_2 immobilized into grape marc-based activated carbon for Rb-5 Azo dye photocatalytic degradation, " Arabian Journal of Chemistry,2015, http://dx.doi.org/10.1016/j.arabjc.2015.06.040.
71. Bahram Ghasemi, Bagher Anvaripour, Sahand Jorfi, and Neematollah Jaafarzadeh, "Enhanced photocatalytic degradation, and Mineralization of Furfural Using

UVC/TiO_2/GAC composite in Aqueous Solution," 2016, Article ID 2782607,http://dx.doi.org/10.1155/2016/278267.

72. Gourab, " Photocatalytic degradation of textile dye using TiO_2-AC nanocomposite," Published by the American Institute of Physics, 2018, https://doi.org/10.1063/1.5038706.
73. M.Asilturk and S.Sener, "TiO_2-activated carbon photocatalysts: Preparation, characterization and photocatalytic activities," *Chem. Eng. J.*, vol. 180, pp. 354–363, 2012, doi:10.1016/j.cej.2011.11.045.
74. Ludek Kaluza, Miroslav Zdrazil, "Slurry Impregnation of ZrO_2 Extrudates: Controlled EggShell Distribution of MoO_3, Hydrodesulfurization Activity, Promotion by Co,"Catal Lett (2009) 127:368–376, DOI 10.1007/s10562-008-9692-1.
75. Arshid M. Ali, Abdulrahim A. Zahrani, "Sequential and/or Simultaneous Wet-Impregnation Impact on the Mesoporous Pt/Sn/Zn/γ-Al_2O_3 Catalysts for the Direct Ethane Dehydrogenation," Journal of Nanomaterials, Volume 2022, Article ID 8739993, 17 pages https://doi.org/10.1155/2022/8739993.
76. George Tsilomelekis, George D. Panagiotou, "Molybdena deposited on titania by equilibrium deposition filtration: structural evolution of oxo–molybdenum (VI) sites with temperature," Phys. Chem. Chem. Phys., 2016, 18, 23980, DOI: 10.1039/c6cp05247a.
77. Peter Munnik, Petra E. de Jongh, and Krijn P. de Jong, "Recent Developments in the Synthesis of Supported Catalysts," Chem. Rev. 2015, 115, 6687−6718, DOI: 10.1021/cr500486u.
78. A.I. Zolotukhina, E.V. Romanova, "Influence of impregnation conditions on the activity of CrOx/Al_2O_3 Catalysts in dehydrogenation of isobutene in fixed bed reactor," Arabian Journal of Chemistry, http://doi.org/10.1016/j.arabjc.2020.10.037.
79. Agnieszka Kołodziejczak-Radzimska, and Teofil Jesionowski, "Zinc Oxide-From Synthesis to Application: A Review," *Materials*,www.mdpi.com/journal/materials, 2014, *7*, 2833-2881; doi: 10.3390/ma7042833.
80. Deraz NM. "The comparative jurisprudence of catalysts preparation methods: I. precipitation and impregnation methods," J Ind Environ Chem. 2018;2(1):19-21.
81. Sarrín, J., "Effect of the preparation method on the reducibility of molybdena- alumina catalysts," *Journal of Molecular Catalysis A: Chemical*, *144*(3), 441–450. https://doi.org/10.1016/S1381-1169(99)00045-X.

82. Vanitha Katheresan, Jibrail Kansedo, Sie Yon Lau, "Efficiency of various recent wastewater dye removal methods: A review," Journal of Environmental Chemical Engineering, https://doi.org/10.1016/j.jece.2018.06.060.
83. Adegboyega Surajudeen Olawale, Olusegun Ayoola Ajayi, Michael Sunday Olakunle, Mku Thaddeus Ityokumbul, and Sam Sunday Adefila, "Preparation of phosphoric acid activated carbons from Canarium Schweinfurthii Nutshell and its role in methylene blue adsorption," Journal of Chemical Engineering and Materials Science, Vol. 6(2), pp. 9-14, July 2015, DOI 10.5897/JCEMS2015.0219.
84. Boonpoke, A., "Study on preparation of water hyacinth-based activated carbon for pulp and paper mill wastewater treatment," Journal of Environmental Biology, Vol. 36, 1143-1148, September 2015, https://doi.org/10.1016/j.jenvman.2021.113477.
85. M. F. Elkady, M. M. Hussein, H. M. Atiaa, "Preparation of Nano-Activated Carbon from carbon Based Material for Copper Decontamination from Wastewater," American Journal of Applied Chemistry. Special Issue: Nano-technology for Environmental Aspects. Vol. 3, No. 3-1, 2015, pp. 31-37. doi: 10.11648/j.ajac.s.2015030301.15.
86. S. Rengaraj, S. H. Moon, R. Sivabalan, B. Arabindoo, and V. Murugesan, "Agricultural solid waste for the removal of organics: Adsorption of phenol from water and wastewater by palm seed coat activated carbon," *Waste Manag.*, vol. 22, no. 5, pp. 543–548, 2002, doi: 10.1016/S0956-053X(01)00016-2.
87. Soegiarto Adi Soenjaya, Nova Handoyo, Felycia Edi Soetaredjo, Artik Elisa Angkawijaya, Yi-Hsu Ju, Suryadi Ismadj " Preparation of carbon fiber from water hyacinth liquid tar " Int J Ind Chem (2015) 6:1–7, DOI :10.1007/s40090-014-0026-4.
88. Rita Bonfiglio, Elena Bonanno, "Energy Dispersive X-ray (EDX) microanalysis: A powerful tool in biomedical research and diagnosis", European Journal of Histochemistry; volume 62: 2841.
89. Roula Abi Saad1, Ghassan Younes, Mohammad H. El-Dakdouki, and Rami Al-Oweini, "Vanadium-Substituted Polyoxomolybdates for Methylene Blue Adsorption from Aqueous Solutions," Journal of Cluster Science, 2021, https://doi.org/10.1007/s10876-021-02130-4.
90. Abraham Balew, "Synthesis and Performance Evaluation of Titanium dioxide supported bentonite composite for methyl orange removal from wastewater," School of Chemical Engineering, MSc thesis, 2019, University of Addis Ababa Institute of Technology.

91. Bahram Ghasemi, Bagher Anvaripour, Sahand Jorfi,and Neematollah Jaafarzadeh, "Enhanced Photocatalytic Degradation and Mineralization of Furfural Using UVC/TiO2/GAC Composite in Aqueous Solution," International Journal of Photoenergy Volume 2016, Article ID 2782607, 10 pages http://dx.doi.org/10.1155/2016/2782607.
92. P.Gonzale-Garcia, "Preparation of activated carbon from water hyacinth stem by chemical activation with K_2CO_3 and its performance as adsorbent of sodium naproxen," Environmental Progress and Sustainable Energy,doi:10.1002/ep.13366, 2019.
93. Jonelle Cornette, "Enviromentally Sustainable Management of Water Hyacinth (Eichhornia Crassipes)," in Guyana International Journal of Agriculture and Forestry 2018,8(1): 4-9, DOI:10.5923/ijaf.20180801.02.
94. Ephraim Vunain, "Characterization of Activated Carbon Prepared from Low-rank Coal of East Kalimantan by using Acid and Base Activation," DOI:10.5220/0010021901780181.
95. Ephraim Vunain, " Synthesis and characterization of low-cost activated carbon prepared from Malawian baobab fruit shells by H3PO4 activation for removal of Cu(II) ions equilibrium and kinetics studies, " Appl Water Sci, 2017, DOI:10.1007/s13201-017-0573-x.
96. Karen L. "Production and characterization of low-cost activated carbon from coal for gold adsorption in cyanide solutions, " vol.40 NO.4, 2020, Doi: http://dx.doi.org/10.1007/s13201-017-0573-x.
97. Elisabeth Schroder, "Experiments on the generation of activated carbon from biomass,"J.Anal. Appl. Pyrolysis 79(2007) 106-111.
98. Daniel Kibami, "Preparation and characterization of activated carbon from Fagopyrum esculentum Monench by H_3PO_4 and HNO_3 chemical activation, " Pelagia Research Librarey,2014.
99. Yakout SM, "Characterization of activated carbon prepared by phosphoric acid activation," Arabian Journal of Chemistry 9, 2016.
100. S Maulina, "Characteristics of activated carbon resulted from pyrolysis of the oil palm fronds powder", Materials Science and Engineering 309 (2018) 012072, doi:10.1088/1757-899X/309/1/012072.
101. Jagtoyen M, "Activated carbons from yellow poplar and white oak by H_3PO_4 activation", *Carbon, Science Direct* 36.

102. Jagtoyen M, Derbyshire, “Activated carbons from yellow poplar and white oak by H3PO4 activation”, Science Direct 36 7-8.

103. Bahram Ghasemi, “Enhanced Photocatalytic Degradation and Mineralization of Furfural Using UVC/TiO_2/GAC Composite in Aqueous Solution", Volume 2016, Article ID 2782607, http://dx.doi.org/10.1155/2016/2782607.

104. Alessandro C. Martins, “Sol-gel synthesis of new TiO_2/activated carbon photocatalyst and its application for degradation of tetracycline”, Ceramics International, doi: http://dx.doi.org/10.1016/j.ceramint.2016.12.088.

105. Xin Zheng, “Adsorption Properties of Granular Activated Carbon-Supported Titanium dioxide supported Particles for Dyes and Copper Ions”, 2018, doi: 10.1038/s41598-018-24891-1.

106. Xiaojing Wang," Degradation of methyl orange by composite photocatalysts nano-TiO_2 immobilized on Activated carbons of different porosities", Journal of Hazardous Materials 169 (2009) 1061–1067," doi: 10.1016/j.jhazmat.2009.04.058.

107. Xiaojing Wang, Yafei Liu, Zhonghua Hu, Yujuan Chen,Wei Liu, Guohua Zhao, " Degeradtion of Methyl Orange by composite photocatalyst nano-TiO_2 Immobilized on Activated Carbons of different porosities, " Journal of Hazardous Materials, 2009, doi: 10.1016/j.jhazmat.2009.04.058.

108. Juergen Hahn, Thomas F. Edgar, " An improved method for nonlinear model reduction using balancing empirical Grampians, Computers and Chemical Engineering 26 (2002) 1379– 1397.

109. Mohammad, S., et al., "Synthesis, characterization, and application of ZnO-Ag as nano-photocatalyst for organic compound degradation...," J. Environ. Sci. (2015), http://dx.doi.org/10.1016/j.jes.2015.03.030.

110. Khan Mamun Reza, Asw Kurny, and Fahmida Gulshan, " Parameters affecting the photocatalytic degradation of dyes using TiO_2: a review", Appl Water Sci, 2015, doi: 10.1007/s13201-015-0367-y.

111. A. Khataee, S. Arefi-Oskoui “Sonochemical synthesis of Pr-doped ZnO nanoparticles for sonocatalytic degradation of Acid Red 17,” Ultrasonic Sonochemistry, vol. 22, pp. 371–381, 2015.

112. Nimra Nadeem, Muhammad Zahid, Asma Tabasum, Asim Mansha, Asim Jilani, Ijaz Ahmad Bhatti, and Haq Nawaz Bhatti, "Degradation of reactive dye using heterogeneous Photo-Fenton catalysts: $ZnFe_2O_4$ and GO-$ZnFe_2O_4$ composite", Mater. Res. (2020) 015519, https://doi.org/10.1088/2053-1591/ab66ee.

113. Afshin Ebrahimi, Negar Jafari, Karim Ebrahimpour, Ali Nikoonahad, Amir Mohammad, Farzad Fanaei, "The performance of TiO_2/NaY-zeolite nanocomposite in photocatalytic degradation of Microcystin-LR from aqueous solutions: Optimization by response surface methodology (RSM)", Environmental Health Engineering and Management Journal 2020, 7(4), 245–256, doi:10.34172/EHEM.2020.29.

114. Shaban, M., Abukhadra, M. R. & Hamd, A. "Recycling of glass in synthesis of MCM-48 mesoporous silica as catalyst support Ni_2O_3 photocatalyst for Congo red dye removal." *Clean Technol. Environ. Policy,* 2017, https://doi.org/10.1007/s10098-017-1447-5.

APPENDIX A: Proximal analysis

i. Moisture contents

The oven-dried four grams of WHS was measured and taken in a petri dish. It was dispersed nicely on the petri dish. It was then heated at 105℃ for 12hr. The petri-dish was left open during the heating process. After heating, the petri-dish was cooled in a desiccator and then weighed. This specifies the amount of moisture content present in the sample.

$$MC=\frac{W1-W2}{W1}\times 100 \quad \ldots 1.0$$

ii. Ash Content

The oven-dried four grams of activated carbon were measured and taken in a crucible. It was then heated to 650 °C for 3hr. During this test, the crucible was left open. The heating was done in a Nebreathern furnace. After the required heating, the crucible was cooled in a desiccator and then weighed. In this test, the amount of residual substance is equal to the ash present in the sample.

$$AC=\frac{Wash}{Ww}\times 100 \quad \ldots 1.1$$

iii. Volatile Content

The oven-dried four grams of sample was measured and placed in a closed crucible. It was then heated up to 900℃ for exactly 7 min in a furnace. The crucible was then cooled in a desiccator and weighed. The weight of the sample before heating and after heating was used to determine the amount of volatile matter present in the sample.

$$VM=\frac{Wd-Wash}{Ww}\times 100 \quad \ldots 1.2$$

iv. Fixed Carbon

The fixed carbon content is determined by subtracting the sum of percentage compositions of moisture content, volatile matter content, and ash content form 100. The value obtained is the amount of fixed carbon present in the sample expressed in percentage.

$$FC = 100 - (MC + VM + AC) \quad \ldots 1.3$$

v. AC Yield

Activated carbon yield is the ratio of the weight of the sample after carbonization to the weight before carbonization and it tells us how much of the precursor is changed through the carbonization process. The yield of AC was calculated as the percentage weight of the resultant activated carbon divided by the weight of dried WHS.

Yield (%) = $\frac{\text{WAC}}{\text{WWH}} \times 100$ ……1.4

vi. Bulk Density

The activated carbon sample was packed in a previously weighed 25 cm^3 specific gravity bottle by repeatedly tapping the bottle so that powder is filled up to the mark. The powder was poured into the bottle then, weighed again. The difference in the weights gives the bulk density.

BD= $\frac{\text{weight of powder taken in the bottle}}{25}$ …… 1.5

vii.Moisture analyzer

A moisture analyzer (OHAU, Germany) with a model of (MB45) was used to measure the moisture content of raw WHS, with radiation heat of 100 ℃ for 10min, and finally we will get the moisture content of WHS.

APPENDIX B: Crystallite size calculation for WHAC and TiO_2/WHAcc

$$D = \frac{K\lambda}{\beta COS\theta}$$

Peak postion 2Theta(deg)	FWHM(deg)	Crystallite size	Dnm(Average)
7.6796	0.55	14.47665918	16.38162
13.7191	0.28	28.57701764	
15.2542	0.56	14.31285804	
15.9025	0.1	80.21405802	
18..2378	0.7	#NAME?	Crystalite size of activated carbon=16.38162nm
19.2451	1.12	7.194337174	
20.5014	1.12	7.208168197	
21.6583	0	#DIV/0!	
23.1149	1.08	7.508054157	
24.2225	0.86	9.447834707	
25.0709	0	#DIV/0!	
26.6482	1.24	6.583910237	
27.5867	0	#DIV/0!	
28.046	1.04	7.873377628	
29.1245	0	#DIV/0!	
30.4403	0.715	11.51478366	
31.8811	0.16	51.63741041	

APPENDIX C: Synthesis of photo catalyst using microbial hood

APPENDIX D: Absorbance value of the different concentration of MB solution with a calibration plot

Adsorption Experimental Analysis

Plotting the standard curve was important for calculating the final concentration of MB from absorbance which is in return important for calculating the percentage of color removal. For this reason, different MB concentrations (5, 7.5, 10, 12.5, 15 mg L^{-1}) were prepared and their respective absorbance was measured using UV-spectrometer according to the literature. Finally, the linear relationship of absorbance versus concentration of MB was plotted and the equation for the final concentration of MB was found from the slope of the graph.

Table 1.0. Variations of Absorbance with MB concentration

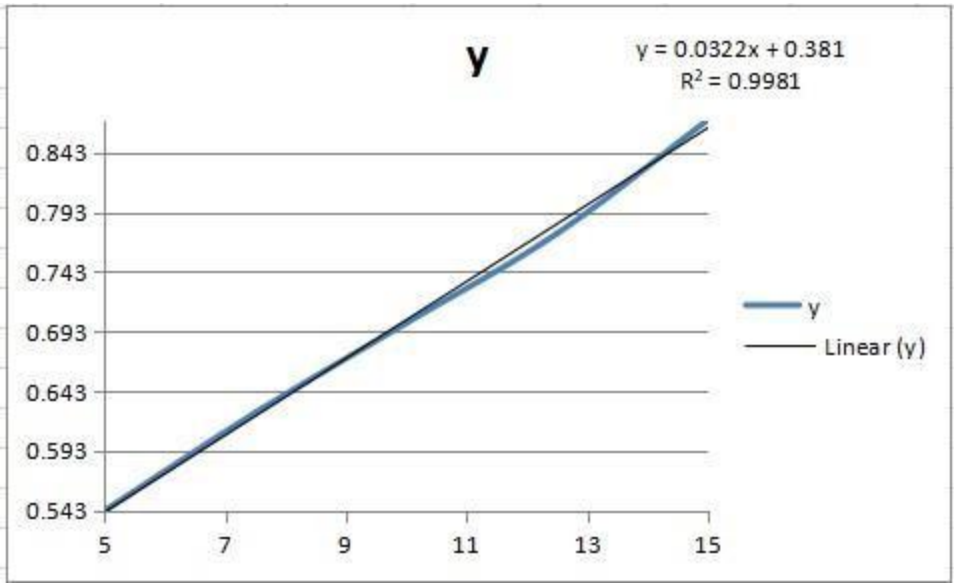

Initial MB concentration in (mg/l)	**Absorbance**
5	0.543
7.5	0.625
10	0.7
12.5	0.775
15	0.87

From the graph, the slope was found to be 0.0322 so that the final equilibrium concentration at any time can be determined by dividing absorbance by that of a slope. Ce= absorbance/0.0322.

Photocatalytic Experimental Analysis

Table 1-1. Variations of Absorbance with MB concentration

Initial MB concentration (mg/L)	Absorbance
10	0.7
15	0.87

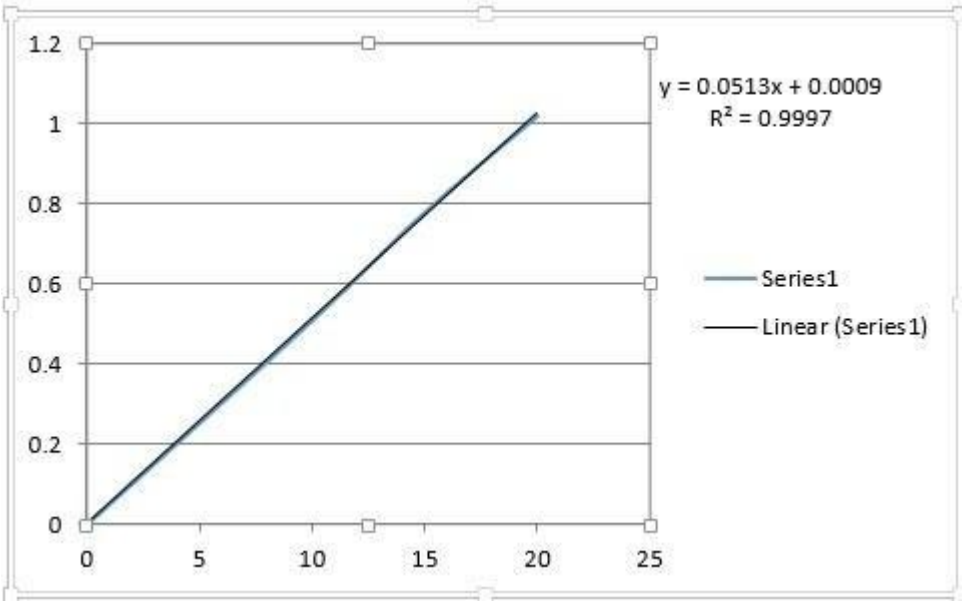

APPENDIX E: FE-SEM with EDX image of WHAC and TiO_2 /WHAcc

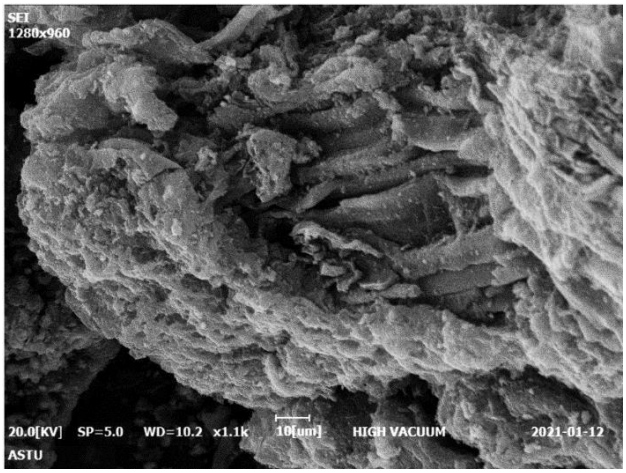

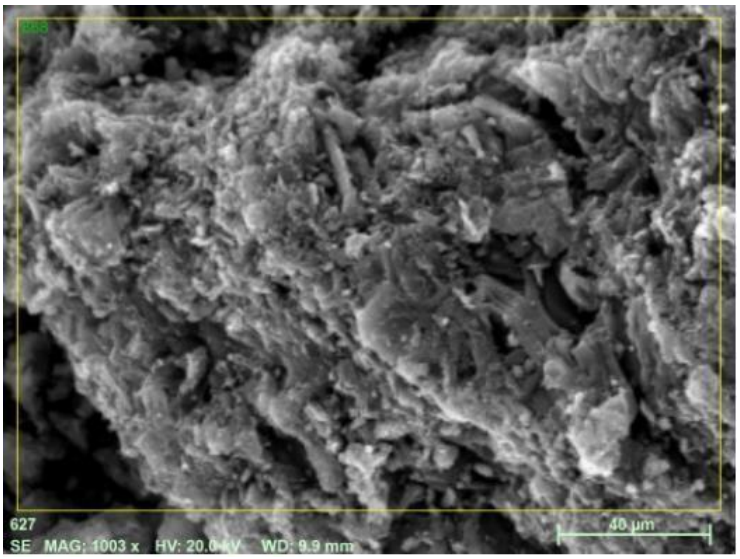

(A)

El	AN	Series	unn. C [wt.%]	norm. C [wt.%]	Atom. C [at.%]	Error (1 Sigma) [wt.%]
C	6	K-series	75.52	75.52	84.48	10.50
O	8	K-series	16.62	16.62	13.96	3.25
Au	79	L-series	4.67	4.67	0.32	0.20
P	15	K-series	2.26	2.26	0.98	0.12
Ti	22	K-series	0.92	0.92	0.26	0.06

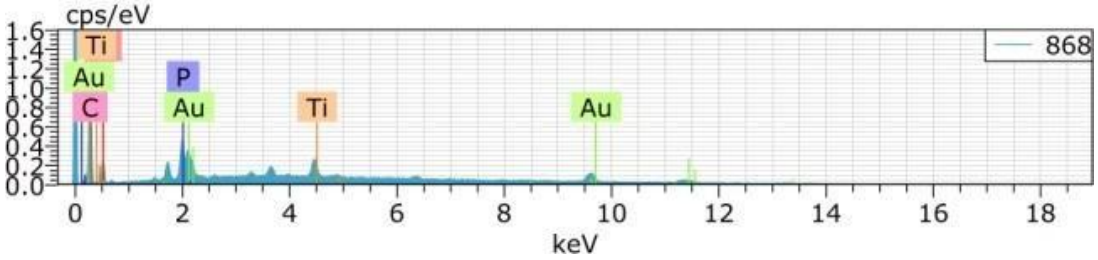

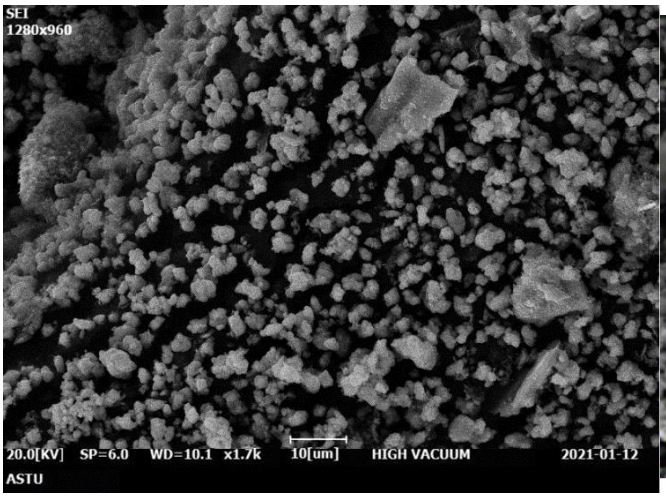

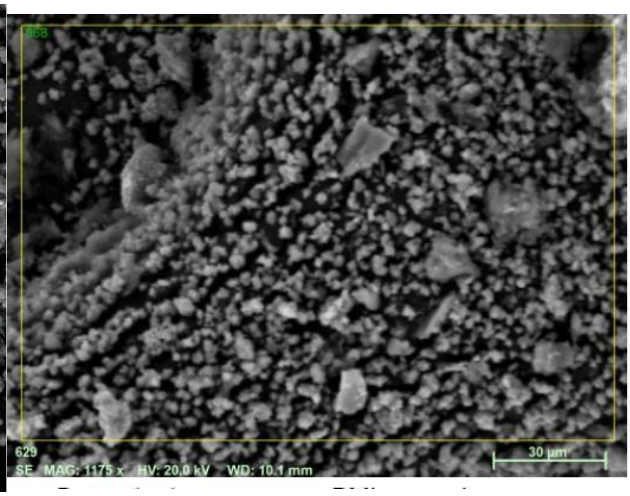

(B)

El	AN	Series	unn. C [wt.%]	norm. C [wt.%]	Atom. C [at.%]	Error (1 Sigma) [wt.%]
O	8	K-series	34.27	51.17	64.77	5.22
Ti	22	K-series	22.20	33.15	14.02	0.65
C	6	K-series	8.29	12.37	20.86	1.61
Au	79	L-series	2.21	3.30	0.34	0.13
P	15	K-series	0.00	0.01	0.00	0.03

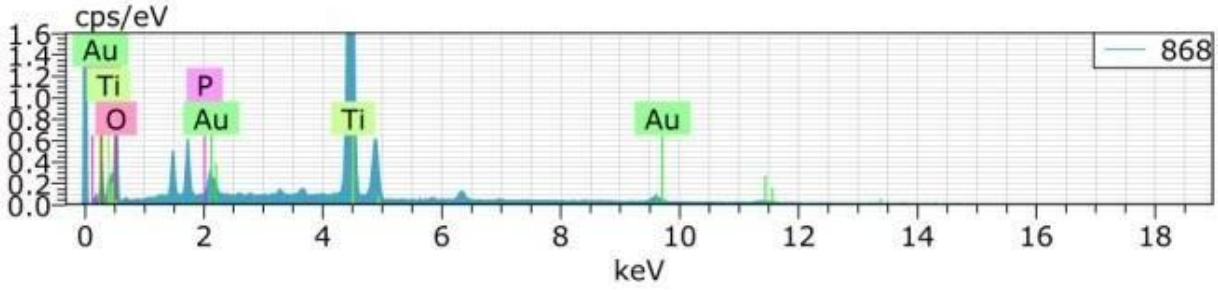

APPENDIX F: Effect of MB concentration on WHAC and TiO_2/WHAcc

Sample	Final dye concentration $c = \frac{A - 0.381}{0.0322}$	Removal efficiency
WHAC (400°C with 25% H_3PO_4)	4.25	71%
WHAC (400°C with 35% H_3PO_4)	2.07	75%
WHAC (400°C with 45% H_3PO_4)	2.1	86%
WHAC (600°C with 25% H_3PO_4)	3.9	73.4%
WHAC (600°C with 35% H_3PO_4)	3.5	76%
WHAC (600°C with 45% H_3PO_4)	0.52	96%
WHAC (800°C with 25% H_3PO_4)	0.590	70%
WHAC (800°C with 35% H_3PO_4)	3	75%
WHAC (800°C with 45% H_3PO_4)	2.08	94%

Sample	Final dye concentration	Removal efficiency
TiO_2/WHAcc for 4 hrs.	2.02	77.8
TiO_2/WHAcc for 8hrs.	1.9317	89.8
TiO_2/WHAcc for 12 hrs.	4.4	90.3

APPENDIX G: Comparison of WHAC and TiO_2/WHAcc

Adsorbent dosage (gm)	Dye concentration (mg/L)	Contact time (min.)	Dye removal WHAC	Efficiency Catalyst
0.093	20	24.336	72.25%	91.05%

APPENDIX H: IR-Spectrum table by Frequency range

Absorption (cm^{-1})	Appearance	Group	Compound Class
3700-3584	medium, sharp	O-H stretching	Alcohol
3550-3200	strong, broad	O-H stretching	Alcohol
3500	Medium	N-H stretching	primary amine
3400-3300	Medium	N-H stretching	aliphatic primary amine
3350-3310	Medium	N-H stretching	secondary amine
3300-2500	strong, broad	O-H stretching	carboxylic acid
3200-2700	weak, broad	O-H stretching	Alcohol
3000-2800	strong, broad	N-H stretching	amine salt
3333-3267	strong, sharp	C-H stretching	Alkyne
3100-3000	Medium	C-H stretching	Alkene
3000-2840	Medium	C-H stretching	Alkane
2830-2695	Medium	C-H stretching	Aldehyde
2600-2550	Weak	S-H stretching	Thiol
2349	Strong	O=C=O stretching	carbon dioxide
2275-2250	strong, broad	N=C=O stretching	Isocyanate
2260-2222	Weak	CΞN stretching	Nitrile
2260-2190	Weak	CΞC stretching	Alkyne
2175-2140	Strong	S-CΞN stretching	Thiocyanate
2160-2120	Strong	N=N=N stretching	Azide
2150		C=C=O stretching	Ketene
2145-2120	Strong	N=C=N stretching	Carbodiimide
2140-2100	Weak	CΞC stretching	Alkyne
2140-1990	Strong	N=C=S stretching	I so thiocyanate
2000-1900	medium	C=C=C stretching	Alleyne
2000		C=C=N stretching	Ketenimine
2000-1650	Weak	C-H bending	aromatic compound
1818	Strong	C=O stretching	Anhydride
1815-1785	Strong	C=O stretching	acid halide
1800-1770	Strong	C=O stretching	conjugated acid halide
1775	Strong	C=O stretching	conjugated anhydride
1770-1780	Strong	C=O stretching	vinyl / phenyl ester

1750-1735	Strong	C=O stretching	δ-lactone
1745	Strong	C=O stretching	Cyclopentanone
1740-1720	Strong	C=O stretching	Aldehyde
1730-1715	Strong	C=O stretching	α, β-unsaturated ester
1725-1705	Strong	C=O stretching	aliphatic ketone
1720-1706	Strong	C=O stretching	carboxylic acid
1710-1680	Strong	C=O stretching	conjugated acid
1710-1685	Strong	C=O stretching	conjugated aldehyde
1690	Strong	C=O stretching	primary amide
1690-1640	medium	C=N stretching	imine / oxime
1685-1666	Strong	C=O stretching	conjugated ketone
1680	Strong	C=O stretching	secondary amide
1680	Strong	C=O stretching	tertiary amide
1650	Strong	C=O stretching	δ-lactam
1678-1668	Weak	C=C stretching	Alkene
1675-1665	Weak	C=C stretching	Alkene
1675-1665	Weak	C=C stretching	Alkene
1662-1626	medium	C=C stretching	Alkene
1658-1648	medium	C=C stretching	Alkene
1650-1600	medium	C=C stretching	conjugated alkene
1650-1580	medium	N-H bending	Amine
1650-1566	medium	C=C stretching	cyclic alkene
1648-1638	Strong	C=C stretching	Alkene
1620-1610	Strong	C=C stretching	α, β-unsaturated ketone
1550-1500	Strong	N-O stretching	nitro compound
1465	medium	C-H bending	Alkane
1450	medium	C-H bending	Alkane
1390-1380	medium	C-H bending	Aldehyde
1385-1380	medium	C-H bending	Alkane
810 ± 20	strong	C-H bending	1,4-disubstituted or
780 ± 20	strong	C-H bending	1,2,3-trisubstituted
755 ± 20	strong	C-H bending	1,2-disubstituted

APPENDIX I: Pictures of sample and some laboratory equipment

APPENDIX J: BET-BJH results for WHAC and TiO_2/WHAcc

Quantachrome NovaWin - Data Acquisition and Reduction
for NOVA instruments
©1994-2010, Quantachrome Instruments
version 11.0

Analysis		Report	
Operator:alex	Date:2021/06/28	Operator:alex	Date:6/28/2021
Sample ID: fifi ac aa	Filename:	C:\QCdata\Physisorb\sttn_B_20210627 fifi 10 aa.qps	
Sample Desc:	Comment:		
Sample weight: 0.02 g	Sample Volume: 0.005128 cc	Sample Density:3.9 g/cc	
Outgas Time: 16.0 hrs	OutgasTemp: 300.0 C		
Analysis gas: Nitrogen	Bath Temp: 77.3 K		
Press. Tolerance:0.100/0.100 (ads/des)	Equil time: 60/60 sec (ads/des)	Equil timeout: 240/240 sec (ads/des)	
Analysis Time: 83.0 min	End of run: 2021/06/28 12:05:10	Instrument:	Nova Station B
Cell ID: 2		F/W version:	0.00
t-Method	Calc. method: de Boer		
BJH/DH method	Moving pt. avg.: off	Ignoring P-tags below 0.35 P/Po	
Adsorbate	Nitrogen	Temperature 77.350K	
	Molec. Wt.: 28.013 g	Cross Section: 16.200 Å²	Liquid Density: 0.808 g/cc
	Contact Angle: 0.0 degrees	Surf. Tension: 8.850 erg/cm²	

Radius	Pore Volume	Pore Surf Area	dV(r)	dS(r)	dV(logr)	dS(logr)
Å	cc/g	m²/g	cc/Å/g	m²/Å/g	cc/g	cc/g
36.4346	5.4508e-01	2.9921e+02	2.0976e-02	1.1514e+01	1.6824e+00	9.2355e+02
508.1102	9.2006e-01	3.1397e+02	4.0877e-04	1.6090e-02	2.9038e-01	1.1430e+01

BJH adsorption summary

Surface Area =	313.969 m²/g
Pore Volume =	0.920 cc/g
Pore Radius Dv(r) =	36.435 Å

Quantachrome NovaWin - Data Acquisition and Reduction
for NOVA instruments
©1994-2010, Quantachrome Instruments
version 11.0

Analysis		Report	
Operator:alex	Date:2021/06/28	Operator:alex	Date:6/28/2021
Sample ID: fifi ac aa	Filename:	C:\QCdata\Physisorb\sttn_B_20210627 fifi 10 aa.qps	
Sample Desc:	Comment:		
Sample weight: 0.02 g	Sample Volume: 0.005128 cc	Sample Density:3.9 g/cc	
Outgas Time: 16.0 hrs	OutgasTemp: 300.0 C		
Analysis gas: Nitrogen	Bath Temp: 77.3 K		
Press. Tolerance:0.100/0.100 (ads/des)	Equil time: 60/60 sec (ads/des)	Equil timeout: 240/240 sec (ads/des)	
Analysis Time: 83.0 min	End of run: 2021/06/28 12:05:10	Instrument:	Nova Station B
Cell ID: 2		F/W version:	0.00
t-Method	Calc. method: de Boer		
BJH/DH method	Moving pt. avg.: off	Ignoring P-tags below 0.35 P/Po	
Adsorbate	Nitrogen	Temperature 77.350K	
	Molec. Wt.: 28.013 g	Cross Section: 16.200 Å²	Liquid Density: 0.808 g/cc
	Contact Angle: 0.0 degrees	Surf. Tension: 8.850 erg/cm²	

Radius	Pore Volume	Pore Surf Area	dV(r)	dS(r)	dV(logr)	dS(logr)
Å	cc/g	m²/g	cc/Å/g	m²/Å/g	cc/g	cc/g
36.4346	5.4508e-01	2.9921e+02	2.0976e-02	1.1514e+01	1.6824e+00	9.2355e+02
508.1102	9.2006e-01	3.1397e+02	4.0877e-04	1.6090e-02	2.9038e-01	1.1430e+01

BJH adsorption summary

Surface Area =	313.969 m²/g
Pore Volume =	0.920 cc/g
Pore Radius Dv(r) =	36.435 Å